Geophysical Journal International

Geophys. J. Int. (2012) **190,** 131–150 doi: 10.1111/j.1365-246X.2012.05506.x

Three dimensional lithospheric structure of the western continental margin of India constrained from gravity modelling: implication for tectonic evolution

K. Arora,[1] V. M. Tiwari,[1] B. Singh,[1] D. C. Mishra[1] and I. Grevemeyer[2]

[1]*National Geophysical Research Institute, Uppal Road, Hyderabad* 500007, *India. E-mail: kusumita@ngri.res.in*
[2]*GEOMAR, Helmholtz Centre of Ocean Research Kiel, Düsternbrooker Weg* 20, D-24105 *Kiel, Germany*

Accepted 2012 April 16. Received 2012 April 9; in original form 2011 January 1

SUMMARY

This paper describes a 3-D lithospheric density model of the Western Continental Margin of India (WCMI) based on forward modelling of gravity data derived from satellite altimetry over the ocean and surface measurements on the Indian peninsula. The model covers the north-eastern Arabian Sea and the western part of the Indian Peninsula and incorporates constraints from a wide variety of geophysical and geological information. Salient features of the density model include: (1) the Moho depth varying from 13 km below the oceanic crust to 46 km below the continental interior; (2) the lithosphere–asthenosphere boundary (LAB) located at depths between 70 km in the southwestern corner (under oceanic crust) and about 165 km below the continental region; (3) thickening of the crust under the Chagos–Laccadive and Laxmi Ridges and (4) a revised definition of the continent–ocean boundary.

The 3-D density structure of the region enables us to propose an evolutionary model of the WCMI that revisits earlier views of passive rifting. The first stage of continental-scale rifting of Madagascar from India at about 90 Ma is marked by relatively small amounts of magmatism. A second episode of rifting and large-scale magmatism was possibly initiated around 70 Ma with the opening of the Gop Rift. Subsequently at around 68 Ma, the drifting away of the Seychelles and formation of the Laxmi Ridge was a consequence of the down-faulting of the northern margin. During this second episode of rifting, the northern part of the WCMI witnessed massive volcanism attributed to interaction with the Reunion hotspot at around 65 Ma. Subsequent stretching of the transitional crust between about 65 and 62 Ma formed the Laxmi Basin, the southward extension of the failed Gop Rift. As the interaction between plume and lithosphere continued, the Chagos–Laccadive Ridge was emplaced on the edge of the nascent oceanic crust/rifted continental margin in the south as the Indian Plate was moving northwards.

Key words: Gravity anomalies and Earth structure; Continental margins: divergent; Dynamics: gravity and tectonics; Hotspots; Indian Ocean.

1 BACKGROUND AND OBJECTIVES

The structural fabric of the Western Continental Margin of India (WCMI) contains the signatures of the tectonic history of the Indian subcontinent, its breakup during continental rifting and its magmatic history. A volcanic origin for the WCMI is commonly ascribed as it bears evidence of large-scale magmatic activity related to the Reunion hotspot. The formation of the WCMI occurred in two steps, producing a non-volcanic margin with normal melt generation in the south during the breakup of Madagascar from western India (Storey *et al.* 1995) and a volcanic continental margin with excessive melt generation in the north (White & McKenzie 1989). The large amounts of melt generated in the northern part of WCMI appear to be the consequence of the interaction of the hotspot with thinned lithosphere (Armitage *et al.* 2010). The Deccan volcanism in this region and the subsequent formation of the Chagos–Laccadive Ridge to the south was caused by a deep-seated hotspot. The hotspot is currently located under the island of Reunion, several thousand kilometres from India. The nature of several prominent features offshore from the Deccan Volcanic Province, namely the Laxmi Ridge and the Laxmi Basin, is poorly understood. The Laxmi Ridge is believed to be a fragment of continental crust (Talwani & Reif 1998). The Laxmi Basin to the east of the Laxmi Ridge is either suggested to be the locus of an extinct spreading centre (Bhattacharya *et al.* 1994; Talwani & Reif 1998) or it may be stretched and reworked

continental crust (Miles *et al.* 1998; Todal & Eldholm 1998; Krishna *et al.* 2006).

Numerous works document the geodynamics of the western margin (Whiting *et al.* 1994; Chaubey *et al.* 2002; Radha krishna *et al.* 2002). However, the debate about its breakup history and the nature of lithospheric properties continues (Naini & Talwani 1982; Bhattacharya *et al.* 1994; Miles *et al.* 1998). In this study, we have conducted 3-D modelling of gravity anomalies, constrained by published seismic information, to delineate lithospheric density variations produced by geodynamic processes. We have attempted to incorporate both small-scale units and deep-seated, large-scale variations within the lithosphere into a single model. Modelling the 3-D structure of land and ocean areas to infer the present configuration of the crust and upper mantle poses unique challenges in model computation and is not commonly attempted. Because both the geometry and the density of the continental and oceanic crust contrast sharply, the gravity response across this boundary tends to dominate the computed field. This then requires that the model area cover a large region, with all the complexities that are implied, around the ocean–continent transition. We believe that a comprehensive 3-D model can define the present-day subsurface features in the entire regional context and that this model can then be examined to decipher the signatures of past tectonic events. Also, the position of the continent-ocean-boundary is defined on the basis of maximum horizontal gradients of the Bouguer anomalies.

2 GEOTECTONIC SETTING

Fig. 1(a) presents the physiographic map of the entire northwestern Indian Ocean for the purposes of reference to the present-day position of regional features like the Seychelles, Mascarene Basin and Reunion Island with respect to the Indian landmass; the red box marks the current study region. The location of Deep Sea Drilling Program (DSDP) sites and the age contours of the oceanic crust (Müller *et al.* 2001) are marked.

Fig. 1(b) presents the geotectonic setting and physiography of the study region, corresponding to the red box in Fig. 1(a). This region encompasses the eastern part of the Arabian Sea and the western part of the peninsular shield of India, which is a mosaic of various tectonic provinces dating in age from Early Archaean to Late

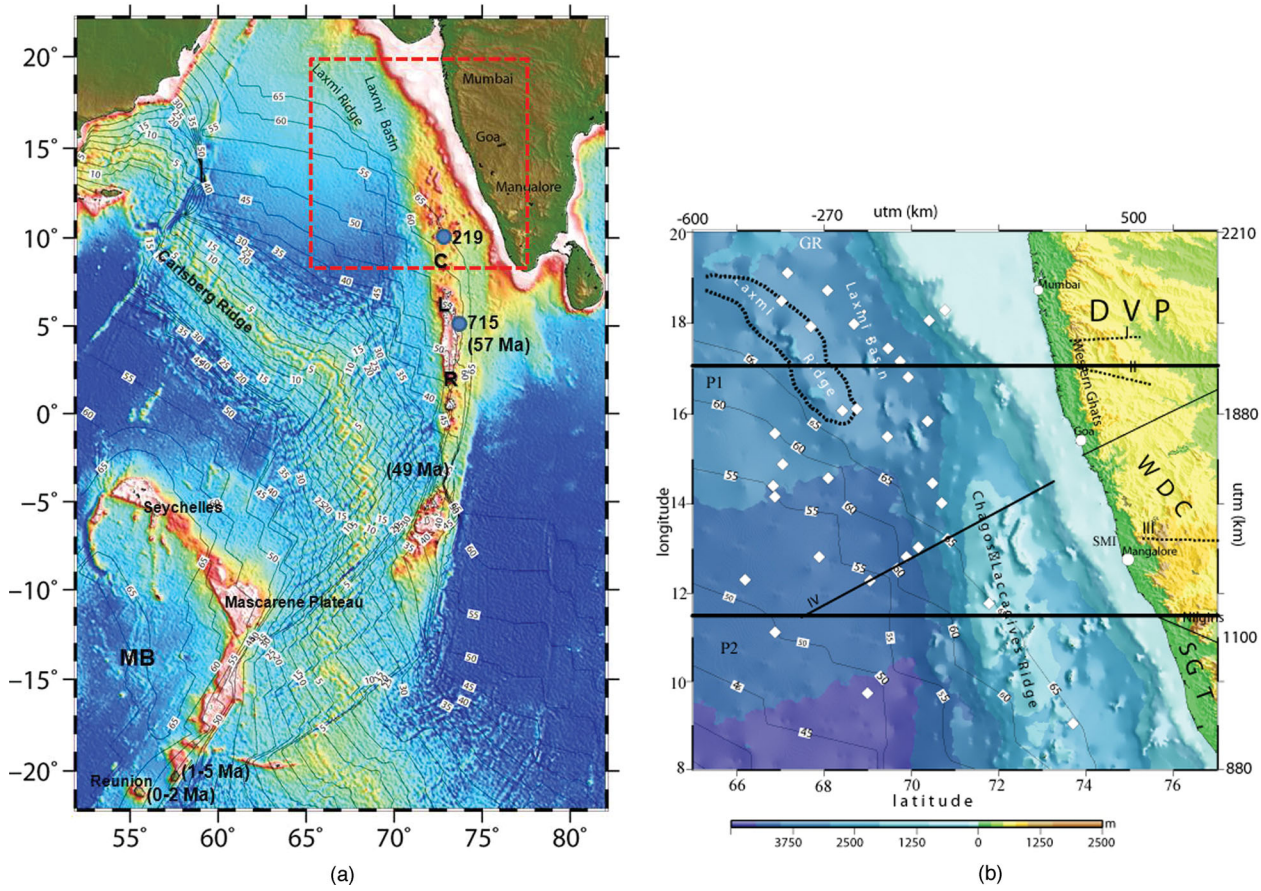

Figure 1. (a) Regional elevation map of the entire region of the northwestern Indian Ocean showing the present day locations of the Seychelles, Carlsberg Ridge, Reunion Islands and Mascarene Basin (MB). The age contours for the oceanic crust are marked for the entire region (Müller *et al.* 2001). The red square marks the outlines of the present study area. The blue circles indicate the locations of DSDP sites. Ages of rocks along the Chagos–Laccadive Ridge and near Reunion are given in brackets (Duncan & Hargraves 1990). (b) Map of the western continental margin of India, showing the three major geological provinces on land and the traces of the main offshore features. Locations of four seismic profiles are marked as I, II, III and IV. I is the Kelsi–Loni deep seismic profile (Kaila *et al.* 1981a), II represents the Guhagar-Chorochi deep seismic profile (Kaila *et al.* 1981b) and III indicates the approximate position of the Kavali–Udipi geotransect, which extends right to the eastern coast (Kaila *et al.* 1979). IV is the refraction profile from Chaubey *et al.* (2002). White diamonds in the Arabian Sea indicate locations of seismic refraction stations. The positions of the two representative vertical sections shown in Figs 4 and 5 are marked as P1 and P2. Contours of age of seafloor derived from magnetic studies are marked (Müller *et al.* 2001). The left and bottom axes show longitude and latitude, whereas the right and top axes provide the corresponding UTM coordinates, Zone 44.

Proterozoic (Kumar *et al.* 1996). Three main geological provinces are marked approximately on land: Deccan Volcanic Province (DVP) in the north, Western Dharwar Craton (WDC) in the central part of the peninsula and the southern high-grade metamorphic terrain (SGT) to the south. The continental shelf along the western margin of India is significantly wider in the north than in the south.

The WCMI and the adjoining Arabian Sea are widely accepted to have formed during Cretaceous intracontinental rifting (Royer *et al.* 1992). Marine magnetic anomalies in the Arabian Sea indicate that at about 104 Ma, Madagascar had separated from Africa but was still attached to India. Towards the end of the Cretaceous Quiet Zone, at about 90 Ma, the spreading axis jumped eastwards and Madagascar separated from India in response to partial melting and doming of the lithosphere, which resulted in passive rifting. This resulted in passive rifting (Pande *et al.* 2001; Storey *et al.* 1995; Subrahmanya 1998). At around 70 Ma, the spreading axis jumped again to the east, following spreading in the Mascarene Basin (MB) and opening of the Gop Rift. At around 68 Ma, micro-continent formation took place as the Seychelles separated from India and transferred to the African plate, whereas seafloor spreading initiated at the Carlsberg ridge (Royer *et al.* 1992; Müller *et al.* 2001). Basaltic magmatism of exceptionally large volumes erupted in the northern part of WCMI in response to rapid rifting under the influence of the Reunion hotspot (White & Mckenzie 1989). This led to the formation of the Deccan Volcanic Province around 65 Ma (Courtillot *et al.* 1986).

Offshore, the WCMI is marked by several prominent aseismic ridges, embankments and volcanic islands. The Chagos–Laccadive Ridge, the Laxmi Ridge and the Laxmi Basin are some of the main features delineated by magnetic, seismic, bathymetry and gravity data in the eastern part of the Arabian Sea. Naini & Talwani (1982), Kolla & Coumes (1990) and Pandey *et al.* (1993) believe that the Laxmi Basin has a transitional crust, while Biswas (1987) and Bhattacharya *et al.* (1994) consider it to be underlain by oceanic crust formed by seafloor spreading; Krishna *et al.* (2006) infer the Laxmi Ridge to be a fragment of stretched continental crust and the Laxmi Basin to be a failed rift, which was further stretched before and during the episode of Deccan volcanism. However, an unequivocal conclusion regarding the nature of the Laxmi Basin is still lacking. Recent results from subsidence analysis suggest more subsidence in the eastern part of Laxmi Basin during the last 20 m.y. This may be interpreted as evidence of continuation of tectonic activity (Whiting *et al.* 1994). On the basis of receiver functions studies, Gupta *et al.* (2003) have suggested the presence of a high-velocity underplated layer below the Laccadive Islands, which may extend right from Reunion Island to the Laxmi Ridge (Naini & Talwani 1982; Gallart *et al.* 1999).

3 GRAVITY ANOMALIES

3.1 Free-air anomaly map

Fig. 2(a) is the free-air anomaly map of the WCMI, prepared from the gravity model derived from satellite altimetry data over the oceanic region (Andersen & Knudsen 2001) and surface measurements over the continent (GMSI 2006). The coastline, the continent–ocean boundary, the outline of the Laxmi Ridge, magnetic anomaly lineations, positions of offshore seismic refraction stations and deep seismic profiles on land, as well as the positions of the two representative vertical sections P1 and P2 are marked.

Using the high-density data collected from multisatellite missions, the precision of the derived global gravity fields, available on a 2' by 2' grid, is reported to be of the order of $\sim\pm3$ to ±14 mGal from the comparisons of shiptrack gravity and altimeter-derived gravity measurements (Tapley & Kim 2001). The KMS01 data set is found to give the smallest differences to shipborne gravimetry on an average and is selected for this study on the basis of comparison with available shiptrack gravity data. Because in this work, we have converted the free-air anomalies in offshore areas to Bouguer anomalies, the data used for modelling is smoothed as a result of this conversion. Further, computational limitations restrict the model resolution to about 15 km, hence we felt that the KMS01 data set is suitable and sufficient for our modelling purposes.

The station spacing of onshore surface gravity data ranges between 5 and 10 km and has a variable accuracy of 1–2 mGal, depending on station location and method of height measurements. Regional-scale anomalies are marked on the map, which are intended to indicate the entire trend rather than an isolated anomaly alone. The Laxmi Ridge is marked by prominent gravity low FAl1, whereas the nearly flat seafloor region of the Laxmi Basin is characterized by a broad NW-trending gravity high, FAh1; this signature tapers off to the south at about 16°N. The uncharacteristically wide shelf of the northern part of the margin is marked by the high–low pair FAh2–FAl2, extending as a linear anomaly paralleling the shelf; the shelf itself shows two prominent local variations FAl3 and FAh3 in this area. Such a signature of consistent contrast in gravity anomalies with the high on the landward side and the low to the offshore, is typical of volcanic margins (Menzies *et al.* 2003); similar signatures are reported offshore the west coast of Norway where the Vøring Plateau and Vøring Basin are formed due to rifting along the coast line (Mjelde *et al.* 2007).

Along the coastline, FAl4 extends linearly with magnitudes ranging from -80 to -40 mGal. To the east, the higher topography of the Deccan Volcanic Province (DVP) and the Nilgiris are reflected as FAh4 and FAh5, respectively. In the south, the shelf is significantly narrower; the FAh2–FAl2 pair is extended with more subdued amplitudes, FAl5. To the west, the Chagos–Laccadive Ridge is marked by a chain of isolated gravity highs, FAh6. Further west, the ocean basins exhibit no prominent gravity anomalies.

3.2 Bouguer gravity data

Bathymetry data from the GEBCO database over the Arabian Sea (Intergovernmental Oceanographic Commission 1997) are used to compute the bathymetric corrections offshore. This correction is applied to the grid of free-air anomaly data in offshore areas by computing the 3-D response of the water column (density 1030 kg m^{-3}) and replacing it with rock material (density 2670 kg m^{-3}), which is equal to the Bouguer reduction density used on land over the offshore parts of the model space. The free-air anomalies on the continent are converted to terrain corrected Bouguer anomalies on the basis of surface height measurements. Bathymetric gradients off the coastline, as well as the topography of the Nilgiris, contribute significantly to terrain corrections at stations near the coast.

To bring the two data sets to a common datum, they are converted to UTM coordinates (zone no. 44). Because both the onshore and offshore data are referenced to the WGS84 datum, problems associated with differences in datum were not severe. Along the coast, 25 km to each side of it, the anomalies from the two data sets were manually edited and regridded to generate the seamless Bouguer anomaly map (Fig. 2b).

The work of Bowin (1983) provides initial assessment that long-wavelengths (>4000 km) anomalies are likely due to mass anomalies at the core–mantle boundary and in the lower mantle, probably below 600 km in the lower mantle. The intermediate wavelength

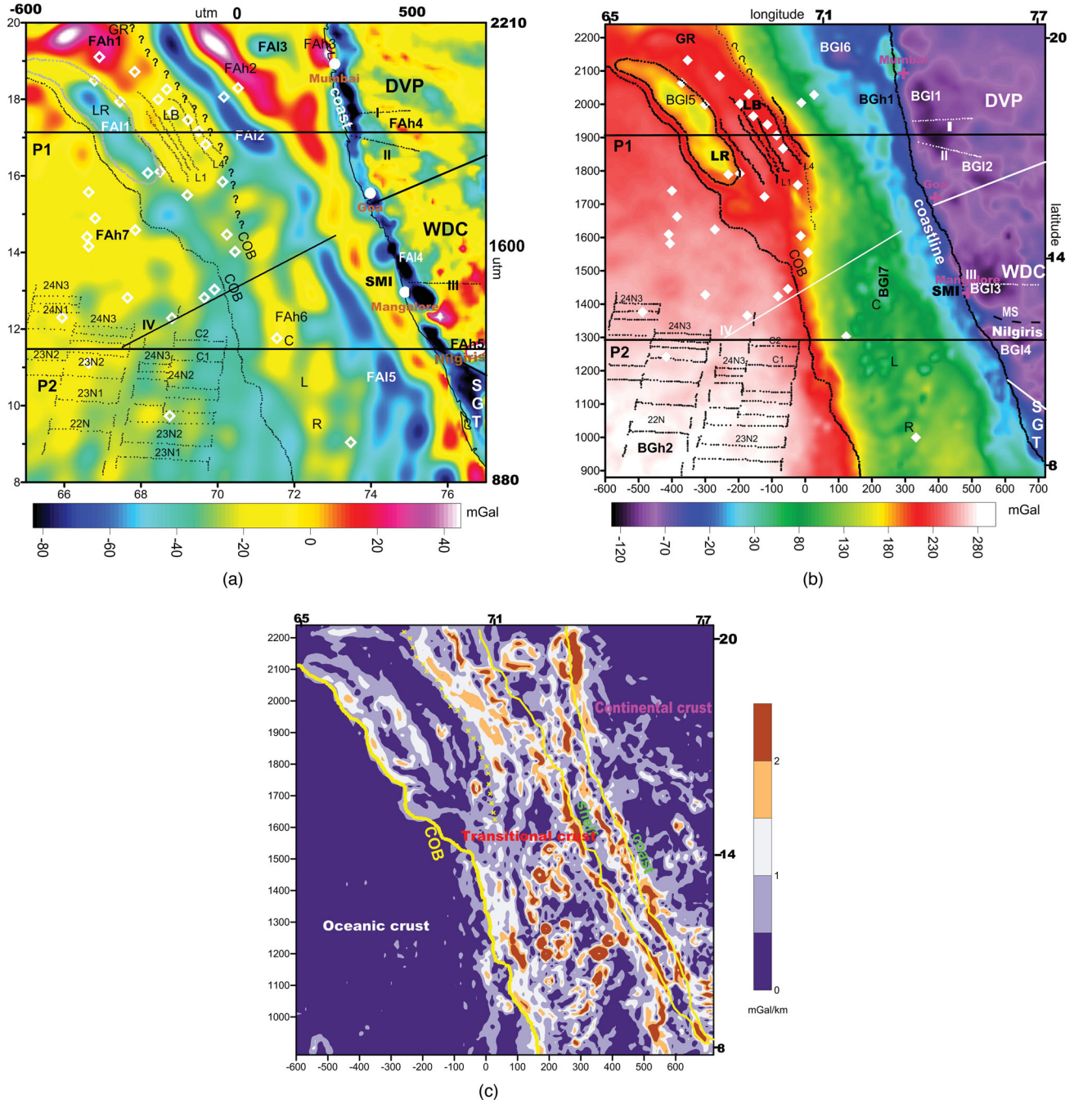

Figure 2. (a) Free-air anomaly map of the study region based on KMS data (Andersen & Knudsen 2001) in offshore areas and surface data on land (Gravity Map Series of India 2006). Magnetic lineations in the Arabian Sea and Laxmi Basin (Kolla & Coumes 1990; Krishna *et al.* 2006), outline of the Laxmi Ridge and the coastline are marked. The geological provinces and positions of offshore seismic refraction stations and deep seismic profiles on land and ocean (I, II, III, IV) as well as the positions of the two representative vertical sections P1 and P2 are marked as in Fig. 1(b). The continent–ocean boundary (COB) is marked based on the computations of maximum horizontal gradients of the Bouguer anomalies (shown in Fig. 2c). Significant anomalies are marked as FAl (low) and FAh (high) on the map and their geological explanations are discussed in the text. A line of '?' marks the possible alternate position of the COB in the north as discussed in text, Section 6.3. (b) Observed Bouguer gravity map of the study region; terrain corrected Bouguer and bathymetric corrections were applied using a correction density of 2670 kg m^{-3}, as described in the text. Magnetic lineations in the Arabian Sea and Laxmi Basin, outline of Laxmi Ridge, the coastline, geological provinces and positions of offshore seismic refraction stations and deep seismic profiles on land and ocean (I, II, III, IV), the positions of the two representative vertical sections P1 and P2 as well as the COB are marked as in Fig. 1(a). Significant anomalies are marked as BGl (low) and BGh (high) on the map and their geological explanations are discussed in the text. MS represents the position of the Moyar Shear Zone. A dotted line with '?' marks the possible alternate position of the COB in the north, as discussed in text, Section 6.3. (c) Total horizontal gradient of the Bouguer gravity field; the thick yellow line follows the line of maximum gradient change and forms the basis for our definition of the COB. Other linear gradients are associated with shelf and coast (thin yellow lines) and a smaller gradient (line of yellow 'x') denotes the alternate COB in the north. Localized gradients are associated with topographic features and underplating of intruded transitional crust.

anomalies (300–4000 km) originate in the lower lithosphere and asthenosphere and only the short wavelength anomalies (20–300 km) are largely due to seabed, basement and Moho topography. Accordingly, a regional field corresponding to degree and order 10 of the spherical harmonic representation of the potential field (corresponding to wavelengths >4000 km) would effectively remove the deep-seated density anomalies. However, the removal of a regional field consisting of a truncated set of harmonics may produce large sidelobes, which will appear as highs and lows spaced at the cut-off wavelength of the filter. To avoid this effect, we used harmonic coefficients 2–25 (corresponding to wavelengths ∼1000 to ∼1400 km) where the coefficients were rolled off smoothly. To window the coefficients, we used a Gaussian function.

3.3 Bouguer anomaly map

The Bouguer Anomaly map of the region (Fig. 2b) depicts a first order overview of the present configuration of the crust and lithosphere. Though numerous studies have been conducted on specific areas of the Arabian Sea and the Indian Peninsula, this study attempts a unique treatment of the margin as a whole. This poses some limitations of presentation due to the very large range of values, but allows the visualization of the features from a holistic perspective. On the map, some well known features are marked to aid proper orientation. On land, the gravity anomaly BGl1, known as the Koyna Low, lies in the Deccan Volcanic Province and is attributed to crustal thickening in response to isostatic compensation of the Western Ghat topography (Tiwari & Mishra 1999; Tiwari *et al.* 2001), whereas the low BGl2, known as the Kaladgi low, is attributed to the presence of low-density sediments (2620 kg m^{-3}) of the Proterozoic basin (Tiwari *et al.* 2001). The most prominent gravity low, BGl3, is observed near the coast, over Hasan, lying in the Western Dharwar Craton, spread out over granite, gneiss and schists. It is attributed to the combined effect of crustal thickening up to 50 km (Gupta *et al.* 2010) and lighter upper crustal material that is dominantly felsic in composition (about 2600 kg m^{-3}) and includes large granitic batholiths, exposed in a few places at the surface farther to the south (Qureshy *et al.* 1967; Krishna Brahmam & Kanungo 1976). BGl4 corresponds to the crustal thickening below the Nilgiris and spreads over a vast gneissic country rock; it is known that a suite of low-density syenite rocks (2620 kg m^{-3}) outcrop in this region (Subrahmanyam & Verma 1981). BGl3 and BGl4 are separated by an E–W relative gravity high (Fig. 2b), which may be caused by crustal thinning along the Moyar Shear Zone (MS) as well as intrusions of high-density rocks into the upper crust, which marks the transition between low grade rocks of the Western Dharwar Craton to high grade rocks of the Southern Granulite Terrain (Mishra *et al.* 2006).

In the adjoining Arabian Sea, progressively higher Bouguer values in the direction of the open ocean are the general trend; the sharp gradient across the continental shelf is very prominent. Relative lows BGl5, BGl6 and BGl7 correspond to the Laxmi Ridge, the sedimentary basin off Mumbai and the Chagos–Laccadive Ridge. The overall gradation of Bouguer values from low over the continent, higher on the shelf region and highest over the deep ocean basin is a reflection of lithospheric changes, in terms of both density and thickness. The continental crust to the west is thicker and more felsic on average, the oceanic crust to the east is thinner and composed of basalts, whereas the transitional crust in between comprises of a mixture of the two along with a gradation in thickness.

Farther offshore, the Bouguer anomalies show the expected increasing trend, towards the deep ocean basin, attributed to the decreasing thickness of the crust. The signatures of the offshore ridges are more subdued here compared to those in Fig. 2(a). The gravity low corresponding to the Laxmi Ridge is attributed to an abrupt crustal thickening below the ridge. The variations in thickness of sediments and magmatic material also contribute to shorter wavelength anomalies. This magmatic material is distributed in the form of extruded Deccan basalts and their offshore continuations, in the form of material underplating the crust and also volcanic material associated with the formation of the Chagos–Laccadive Ridge. A short-wavelength gravity high, BGh1, is observed in the north just off the coastline; its source may be a near-surface localized high-density body. The broad high BGh2, on the other hand, is due to crustal thinning in the deep ocean basin and the shallow depth to the high-density mantle material.

Fig. 2(c) depicts the total horizontal gradient of the Bouguer anomalies. Based on these gradients, the three sections of the crust are clearly discernible: the oceanic crust to the west where hardly any gradients exist, the continental crust to the east, where the gradients correspond to elevation trends and the transitional crust in between where numerous gradients of varying trends and amplitude bear witness to the localized variation in densities and geometries in this section. The western-most edge of these anomalies, which forms a continuous trend, is used to define the continent–ocean boundary. Incidentally, this boundary also matches the area where magnetic anomaly lineations cease to be discernible (compare with Fig. 2b). In the following section, modelling of data indicates that this boundary is also coincidental with variation in crustal and lithospheric thickness.

4 INTERPRETING THE OBSERVED DATA THROUGH 3-D MODELLING

4.1 Modelling strategy

The Interactive Gravity and Magnetic Application System (IGMAS) was utilized for the modelling of the Bouguer gravity data to interpret the measured gravity field [Götze & Lahmeyer 1988; Götze (private communication, 1995); Schmidt & Götze 1998). The computed and measured fields are compared and the model geometry and physical parameters are adjusted to achieve an optimum fit. The software also allows inversion of density parameters with constraints on geometry and vice versa. Manual inversion processes were used to test upper bounds on the densities and depths for each density layer. A horizontal three-layered model based on PREM (Dziewonski & Anderson 1981), consisting of upper crust (2700 kg m^{-3}), lower crust (2900 kg m^{-3}) and upper mantle (3300 kg m^{-3}), averaged over continent and ocean, was used as the background reference model. The topmost layer of the reference model is the upper crust, which extends to 15 km depth, the second layer is lower crust, to 35 km depth, and the last includes the upper mantle and the asthenosphere and continues to the base of the model at a depth of 200 km (Table 1). The study area has an extent of approximately 1200 × 1200 km between 8–20°N latitude and 65–77°E longitude. The model geometry is constructed along 55 equal length and parallel E–W vertical sections and IGMAS then

Table 1. Parameters of the background reference model.

Unit	Density (kg m^{-3})	Depth (km)
Upper crust	2670	0–15
Lower crust	2900	15–35
Upper mantle & Asthenosphere	3300	35–200

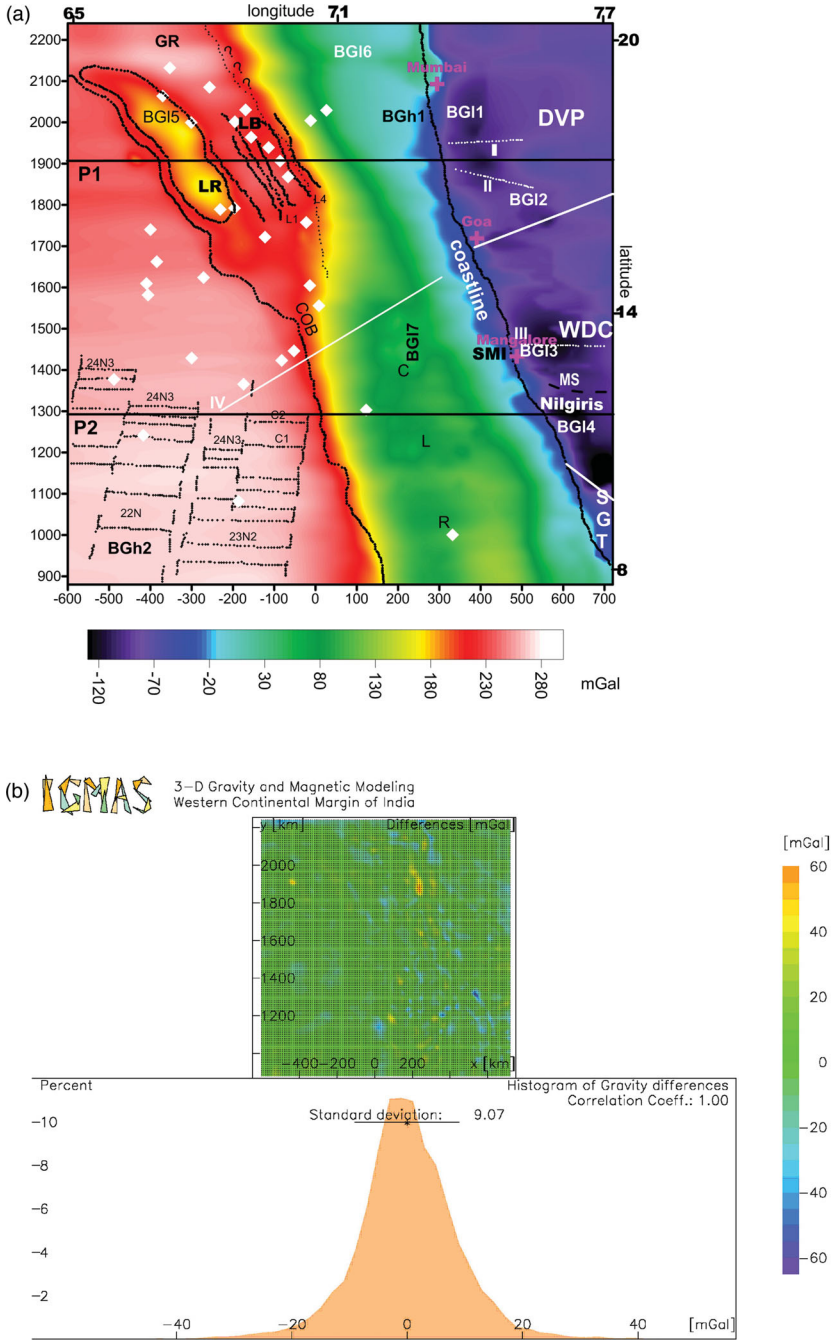

Figure 3. (a) Modelled Bouguer gravity map of the study region. Magnetic lineations in the Arabian Sea and Laxmi Basin, outline of Laxmi Ridge, coastline, geological provinces and positions of offshore seismic refraction stations and deep seismic profiles on land and ocean (I, II, III, IV), the positions of the two representative vertical sections P1 and P2 as well as the COB are marked as in Fig. 1(a). Significant anomalies are marked as BGl (low) and BGh (high), as in Fig. 2(b). MS represents the position of the Moyar Shear Zone. A dotted line with '?' marks the possible alternate position of the COB in the north, as discussed in text. (b) Quantification of the degree of fit between observed and modelled gravity; the correlation coefficient is 1 and the standard deviation histogram shows a near-Gaussian distribution with a maximum value of 9.07 mGal (based on statistical analysis of the differences between observed and calculated Bouguer anomalies from IGMAS).

computes the effect of the entire 3-D body across all of the sections. Thus, there is control on the geometry of structures along the vertical sections; between two consecutive sections, the geometries are defined by automated triangulation. Because the distance between adjacent sections is 25 km, bodies smaller than 15 km in size in the N–S direction are beyond the resolution of the model. Along the E–W sections, resolution is around 10 km. The 3-D response needs to be adjusted iteratively by repeated computations. The response of the accepted model is shown in Fig. 3(a) and compared with the observed Bouguer anomalies.

4.2 Constructing the initial model with constraining information

Seismic velocity data in this region is rather limited. The positions of seismic refraction stations, offshore profiles and onshore deep

seismic profiles are marked in Figs 1 and 2. Some results from seismic tomography and receiver function analyses are also available at selected locations in the Western Dhawar Craton and the Southern Granulite Terrane. More recently acquired seismic reflection data along the coast are not available in the public domain or in published literature. The seismic data, though of variable quality, serve as constraining velocity and depth information and have been used to infer average density values of subsurface bodies using velocity–density relationships from Ludwig *et al.* (1970).

In the north Arabian Sea, average seismic velocities and depths for the different crustal layers are obtained from Naini & Talwani (1982 and references therein) based on a compilation of data from wide-angle seismic reflection and refraction surveys (long- and short-range sonobuoys) and two-ship refraction stations. Structurally, the north Arabian Sea is divided into three major units that include the Laxmi Ridge and the eastern and the western basins on either side. The Moho depth is approximately 22 km under the Laxmi Ridge compared to 12 km and 17 km in the western and the eastern basins, respectively. The top layer, with a velocity of 1.5 km s^{-1}, represents the water column, which is underlain by Tertiary sediments with a velocity of 2.04–2.73 km s^{-1}. Below the sediments, there is a layer with a velocity of 4.46 km s^{-1} under the Laxmi Ridge and the eastern basin, which appears to represent the continuation of the Deccan Traps exposed in western India. This layer is absent under the western basin.

The deeper layers with velocities of 5.51 and 6.67 km s^{-1} in the western basin appear to represent layers 2 and 3, respectively, of the oceanic crust. The layers with velocities of 6.2–6.3 and 7.15–7.19 km s^{-1} under the Laxmi Ridge (Talwani & Reif 1998) and the eastern basin may represent crustal layers, although the latter may also reflect underplated magmatic material (Pandey *et al.* 1993; Singh 1999). An intermediate layer under the Laxmi Ridge and the eastern basin with a velocity of 5.43 km s^{-1} may represent Mesozoic sediments and/or volcanics, but this layer is not consistently seen and it is difficult to constrain its extent.

Records of the Russian expedition of 1975 (Udintsev 1975) show a thick layer beneath the Moho in the central near-shore region that has a velocity of 7.19 km s^{-1}. This suggests the presence of underplated material at the base of the crust towards the southern part of the Arabian Sea and the Chagos–Laccadive Ridge. Seismic refraction studies (Naini & Talwani 1982; Chaubey *et al.* 2002) show that the Moho lies at a depth of 18–19 km, which is deeper than for normal oceanic crust. The crust gradually thins towards offshore areas and is juxtaposed against early Tertiary oceanic crust, 6 km thick, in the Arabian Sea. Drilling at DSDP site 219 (DSDP 1974) at the northern end of the Chagos–Laccadive Ridge suggests that the area is underlain by a layer of velocity 4.0 km s^{-1} overlying one with velocity 5.3 km s^{-1}. Analysis of multichannel seismic reflection, gravity, magnetic and bathymetry data from Ocean Research Vessel (ORV) Sagar Kanya, along a NE–SW regional profile (profile IV in Figs 1 and 2) across the central western continental margin of India has revealed the crustal structure and tectonics of this area (Chaubey *et al.* 2002); 2-D modelling of gravity and magnetic anomalies, constrained by seismic results, reveals 6–27 km thick crust across the margin.

Sediment thickness in the offshore area is adopted from a published sediment thickness map (Divins 1990; Biswas 1987). To aid the definition of the sediment layer in IGMAS, local high-resolution sediment thickness data (Prasada Rao & Srivastava 1984; Parida & Mishra 1992; NGRI Technical Report no. NGRI-2003-EXP-38 (unpublished)) are merged with global sediment thickness data distributed by the NGDC at http://www.ngdc.noaa.gov/mgg/sedthick/sedthick.html.

The constraints used for modelling density structure over the continent come from the results of deep seismic soundings, gravity modelling and perceived tectonics in the region. Deep seismic profiles across the Deccan Volcanic Province, denoted by I and II in Figs 1 and 2 (Kaila *et al.* 1981a,b), pass almost along 17°N and suggests a maximum crustal thickness of 40 km under the Western Ghats that decreases to 35 km on either side. These profiles indicate 2-km-thick Deccan Trap under the Western Ghats, thinning towards the east. A seismic refraction/wide angle reflection study along the Kavali–Udipi profile running coast-to-coast across the shield, denoted by III in Figs 1 and 2, suggests a crustal thickness of 41–42 km under the Western Dharwar Craton, reducing to 34–35 km at the west coast (Kaila *et al.* 1979; Sarkar *et al.* 2001, 2003). Receiver function analyses at 32 sites on the Archaean and Proterozoic terrains of Peninsular India indicate a crustal thickness of 42–51 km beneath the mid Archaean (3.4–3.0 Ga) section of the Western Dhawar Craton (Ravi Kumar *et al.* 2001; Gupta *et al.* 2003).

For constraining the geometry of the bottom of the lithosphere, the general concepts of the oceanic and continental lithosphere have been applied to the initial model. Below the ocean basin at the southwest corner of the model area, the asthenosphere is placed at a depth of 80 km, commensurate with the age of the seafloor in this area. Uniform regional densities of 3300 and 3260 kg m^{-3} have been attributed to the upper mantle and asthenosphere as per recommendations from a profile of gross density of the Earth (PREM; De Bremaecker 1985; Dziewonski & Anderson 1981). Literature has reported localized variations in seismic velocity within the lithosphere of the Dharwar Craton and the Southern Granulite Terrain (Srinagesh & Rai 1996). A low-velocity zone in the upper mantle along the west coast of India is also suggested by Krishna *et al.* (1991) and supported by tomography results (Kennet & Widiyantoro 1999). On the west coast, underplated lower crust along with low velocity upper mantle has also been suggested on the basis of gravity modelling (Mishra *et al.* 2004). However, without ascertaining the spatial extent of these low-velocity zones, including them into the 3-D model would introduce several degrees of uncertainty. Hence, we use uniform densities at greater depths in the model.

The geometry of the lithosphere–asthenosphere boundary is modelled primarily on the basis of the longest wavelength component of the observed gravity field. For visual corroboration of published seismic results within our density model, we have constructed pseudo-velocity logs (different colours delineating the different velocity layers, explained in Table 2) at selected refraction stations in the Arabian Sea as well as at some of the shotpoint locations along the seismic profiles. These logs can be visualized

Table 2. Explanation of the colour codes for the pseudo velocity logs used as constraining information in the 3-D model; the colour coded pseudo-logs are shown in Figs 4 and 5.

Oceanic & transitional crust		Continental crust	
Velocities	Colour code	Velocities	Colour code
<2.0 km s^{-1} 40	Light brown	<5.0 km s^{-1} 90	Red
2.0–4.0 km s^{-1} 50	Light green	5.0–6.0 km s^{-1} 97	Yellow
4.0–5.0 km s^{-1} 60	Pink brown	6.0–6.5 km s^{-1} 100	Light green
5.0–6.0 km s^{-1} 70	Purple	6.5–7.0 km s^{-1} 105	Bright green
6.0–7.0 km s^{-1} 70		7.0–8.0 km s^{-1}	
7.0–8.0 km s^{-1} 80	Chocolate	>8.0 km s^{-1} 110	Cyan
>8.0 km s^{-1}			

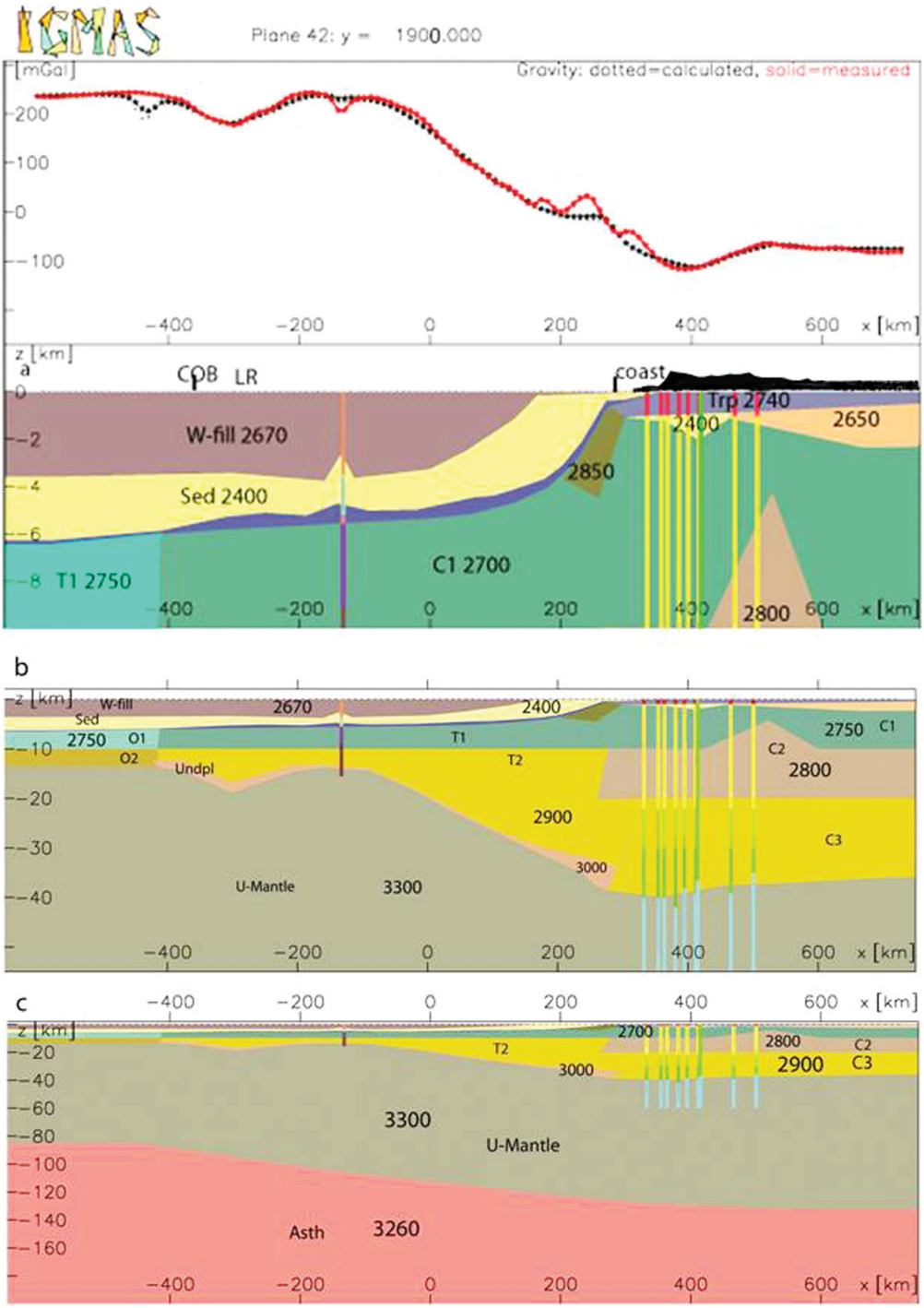

Figure 4. Vertical crustal and lithospheric sections along profile P1, showing depth to (a) 10 km, (b) 55 km and (c) 200 km. In the top-panel, the red is the observed gravity, black is modelled. The names of the density units (Table 3), the densities and positions of constraining seismic information in the form of velocity pseudo-logs (colour code in Table 2) are depicted in the figure. The topography on land, positions of the coastline and the COB are indicated.

in IGMAS by projecting them onto the nearest vertical sections (Figs 4 and 5; projection tolerance 30 km) and the logs then act as a guide to defining the geometry of the layers of the density model.

The model parameters, that is, densities and geometries of each body, were successively modified until an optimum fit was obtained. Fig. 3(b) shows a histogram of gravity differences between observed and calculated values at each grid node in the final model. The correlation coefficient between observed and calculated values is 1 and the standard deviation curve shows a near Gaussian distribution with a peak value of 9.07 mGal, which is acceptable because Bouguer anomalies range from −130 to 300 mGal. The map of differences (Fig. 3b, top-panel) shows short wavelength anomalies, aligned approximately parallel to the margin, which have not been fully modelled with the current configuration. These misfits could

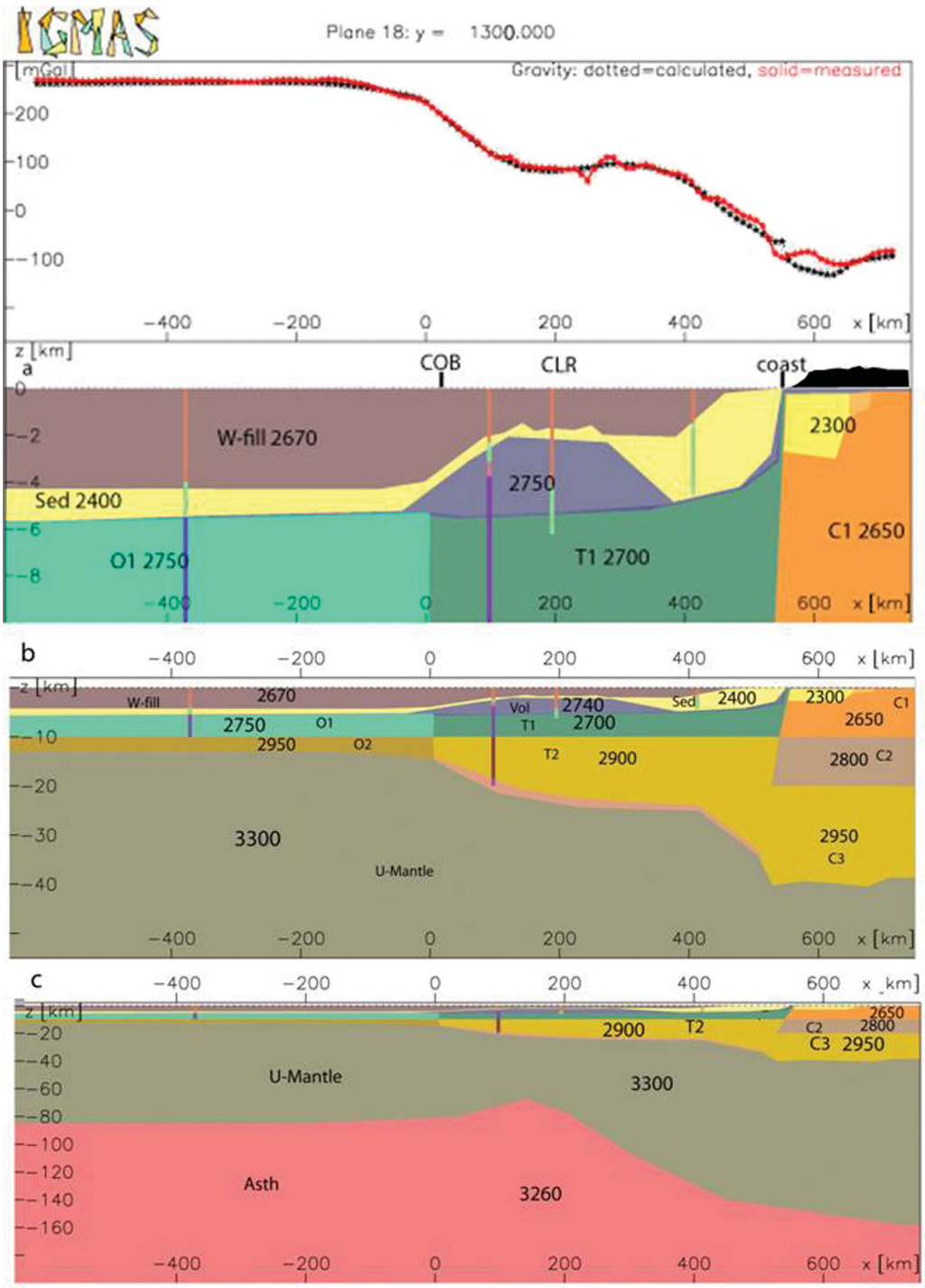

Figure 5. Vertical crustal and lithospheric Section along profile P2, showing depth to (a) 10 km, (b) 55 km and (c) 200 km. In the top-panel, the red is the observed gravity, black is modelled. The names of the density units (Table 3), the densities and positions of constraining seismic information in the form of velocity pseudo-logs (colour code in Table 2) are depicted in the figure. The topography on land, positions of the coastline and COB are indicated.

be improved with better constraints on the smaller, near-surface features in more detailed and localized models.

The 3-D model depicts changes in the distribution of the crust and mantle bodies described above. The geometry of the model is illustrated in two representative sections (P1 and P2 in Figs 1, 4 and 5) and maps of crustal thickness, lithospheric thickness, and thickness of crustal underplating (Figs 6, 7 and 8). Shorter wavelength bodies are not represented in the maps, but they are evident in the two vertical sections shown in Figs 4 and 5. Essentially, the horizontal layers of the initial model were conceptualized in terms of the geometry of a typical rifted margin with the oceanic crust to the west, the continental crust to the east and a transitional zone in between. Table 3 summarizes the constituent units of the density model: the continental crust is differentiated into the upper

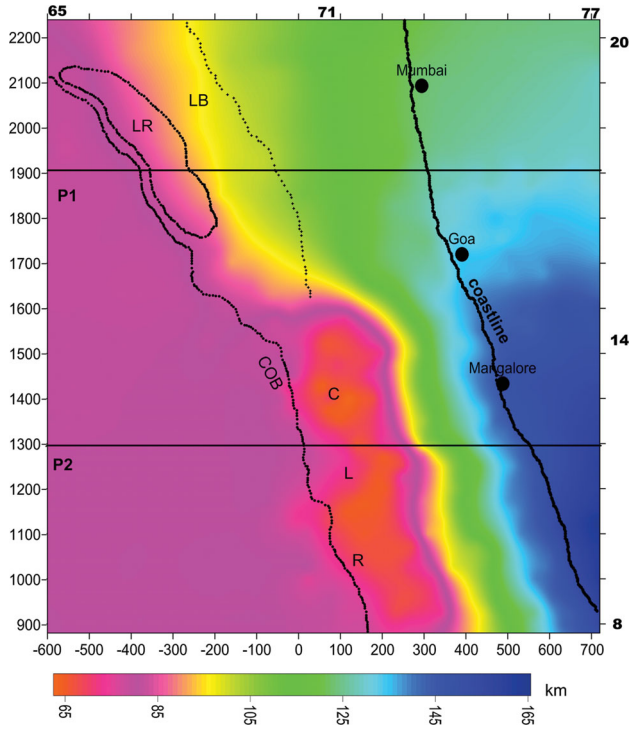

Figure 6. Modelled lithospheric thickness map showing variations in the thickness of the lithosphere from oceanic to cratonic regions across the WCMI from the 3-D density model. The COB, outline of the Laxmi Ridge and Laxmi Basin, coastline and the vertical sections P1 and P2 are marked. The possible alternate position of COB to the east of Laxmi Basin finds no corroboration in the lithosphere-thickness map.

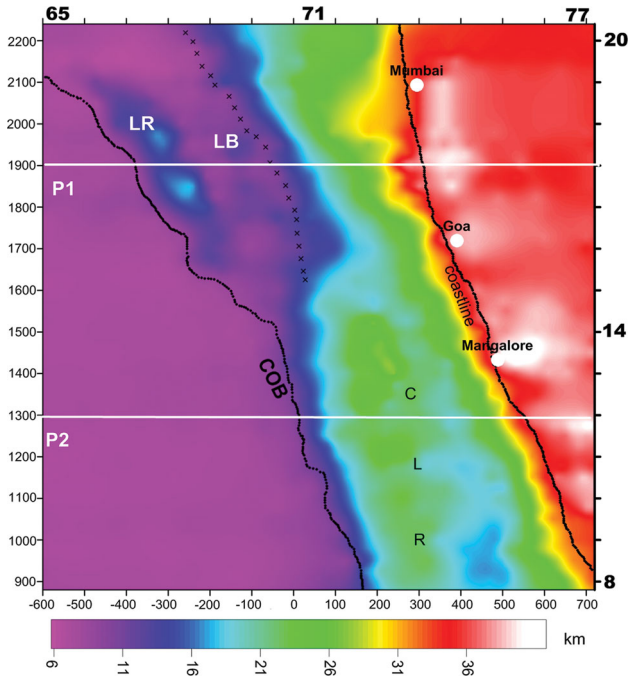

Figure 7. Modelled crustal thickness map, showing the variations in the thickness of the crust from oceanic to cratonic region across the WCMI from the 3-D density model. The crustal thickness does not include the topography on land. COB, outline of Laxmi Ridge and Laxmi Basin, coastline and the vertical sections P1 and P2 are marked. The possible alternate position of COB to the east of Laxmi Basin is plotted by a dotted line and can be correlated with a zone of reduced crustal thickness.

(C1), middle (C2) and lower crust (C3); the transitional and oceanic crusts have two horizontal layers each, T1, T2 and O1, O2, respectively. The upper mantle (U-Mantle) and the asthenosphere (Asth) remain constant in density throughout the model. Und-pl represents the layer of magmatic material underplating the crust and Vol is the volcanic material below the sediment layer (Sed). Trp represents the thin layer of Deccan Traps on the continent, extending offshore and W-fill represents the material used in bathymetric correction with which the oceanic water (of density 1030 kg m^{-3}) is replaced by material with same density (2670 kg m^{-3}) as used for the Bouguer corrections on land.

The southernmost vertical section was referenced to oceanic crust and lithospheric structure (by magnetic lineations) in the west and the rest of the model was subsequently constructed. It may be noted that the density layers deviate in some places from the depths provided by seismic velocity information; this deviation is the result of deliberate changes in geometry made to ensure a fit on adjacent vertical sections to the north and south; herein lies the advantage of a 3-D model.

4.3 Representative vertical sections

Two vertical sections through the model are presented in Figs 4 and 5. The position of the sections is marked in Fig. 1 as P1 and P2, respectively. The two sections depict the model structure in the north and the south at latitudes 17°N and 11.9°N, respectively, Figs 4 and 5 show the subsurface structure at three different scales. The top-panel shows the comparison of the observed and computed gravity anomalies along the chosen sections, below which are sections that depict the geometry of the upper 10 km of crust, the crust and upper mantle to 55 km depth and the entire lithosphere to a depth of 200 km.

4.3.1 Profile P1 (16.9°N; 1900 UTM)

Profile P1 (Fig. 4), which is representative of the northern volcanic part of the margin, shows the geometry of the crustal layers C1, C2, C3, T1, T2, O1 and O2 as described in Section 4.1 and defined in Table 3. A 2-D density profile running across the Arabian Sea, Indian continent and Bay of Bengal, was published by Mishra *et al.* (2004), the results of which are consistent with the geometry on Profile P1. Several pseudo velocity logs along seismic profiles I and II help to define the crustal layers in the western part of the continent and one representative pseudo-velocity log in the Laxmi Basin is placed in the transition zone. The lower surface of the sediment layer is constrained by the global sediment thickness data mentioned in Section 4.2. The oceanic crust consists of parallel layers and the base of the Sed layer lies at 6 km depth on average, which is corroborated by constraining information.

In the west, the Moho lies at a depth of 13 km. Proceeding eastwards, the beginning of the transition zone corresponds to the location of the Laxmi Ridge, which shows a gravity low of about 100 km wavelength. A thin layer (<500 m) of Trp extends into this region from the eruptive site near the coast, where Trp is about 1 km thick. A small rise in the bathymetry at the location of the refraction station is also reflected in the sediments and correlates with a shorter wavelength gravity low.

In the near-shore region, to match an observed gravity high, the modelled thickness of Sed is thinner than the constraints.

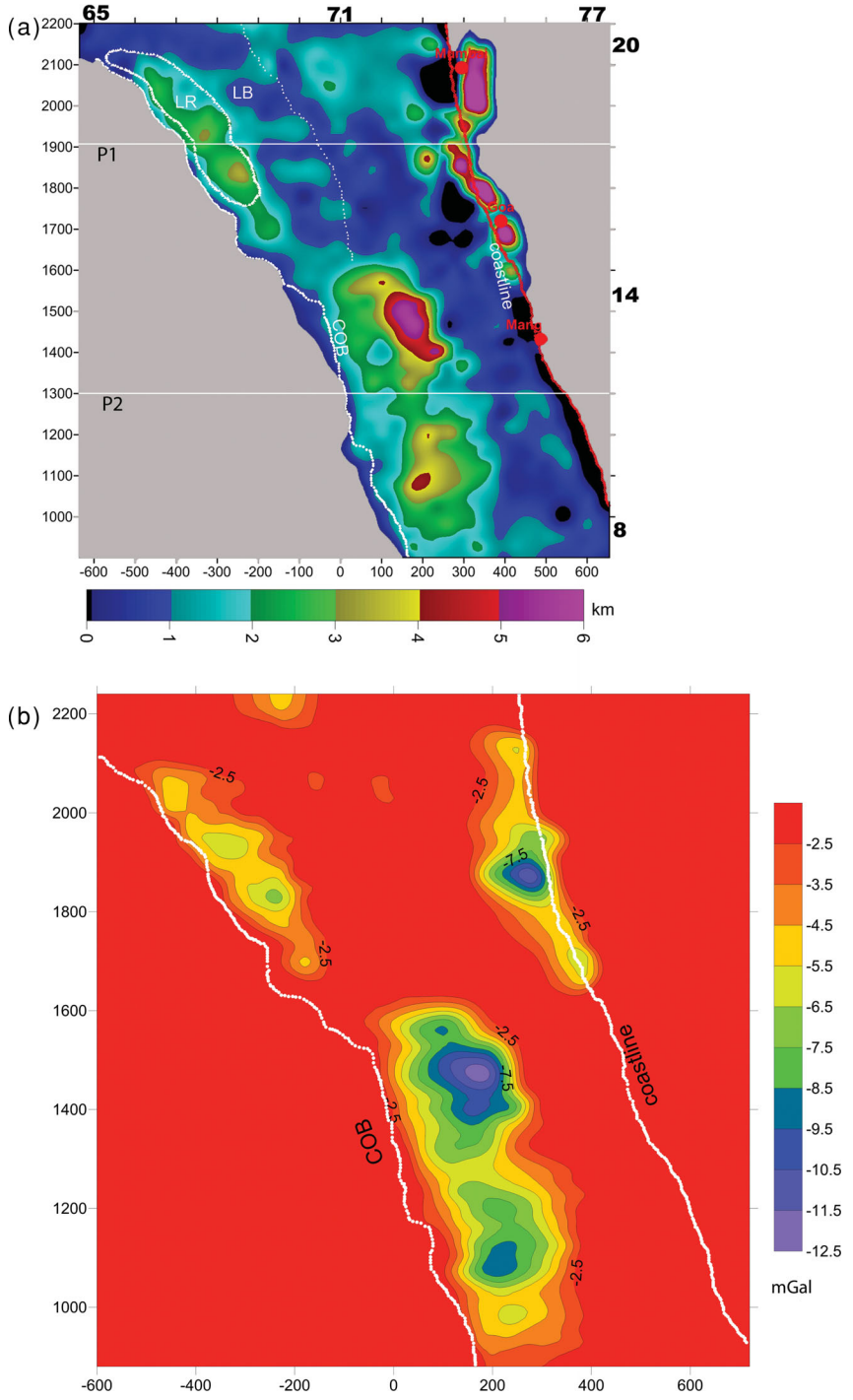

Figure 8. (a) Thickness of underplated material from the 3-D density model. The COB, alternate COB, outline of Laxmi Ridge and Laxmi Basin, coastline and the vertical sections P1 and P2 are marked. (b) Change in model response if the underplated layer at the base of the crust is replaced by lower crustal material.

The prominent gravity high is explained by high density material (2850 kg m^{-3}) below the Trp at the juncture of continental crust. This high-density body also corresponds to accumulation of Und-pl at the crust-mantle boundary; presumably both result from the same episode of volcanic eruption. The existence of this underplated body is not corroborated by recorded velocities, but appears to be a plausible explanation for the gravity high, given that thinning and faulting in response to extensional forces would result in dyke injection and outpouring of magmatic material. The shorter wavelength peaks that are part of the near-shore gravity high remain unaccounted for. This could be attributable to internal variations in geometry and/or density, which is not possible to include in this model.

Und-pl is also about 3 km thick below the Laxmi Ridge, where the Moho dips to 18 km depth and is compensated by a slight basement high below Sed. Though the pseudo-log in Fig. 4 does not show velocities which can be correlated with underplated material, several buoys in the region record velocities of up to 7.4 km s^{-1} (Naini & Talwani 1982), on the basis of which we have continued this layer in vertical sections further to the north. The Moho shallows steeply

Table 3. Bodies used in the construction of the 3-D model and their densities.

Symbol of body	Density in kg m^{-3}	Description of body
W-fill	2670	The water body offshore has been filled with this density
Sed	2250	One layer of sediments has been considered with a representative average density
Trp	2740	represents Traps on land and extension offshore
Vol	2660	represents the volcanic material associated with hotspot interaction in the south
O1	2800	Upper layer of oceanic crust
O2	2900	Lower layer of oceanic crust
T1	2750	Upper layer of transitional crust
T2	2800	Lower layer of transitional crust of intermediate density and representing thinned and stretched continental crust
C1	2700	Upper continental crust
C2	2750	Middle crust
C3	2900	Lower crust
Und-pl	3000	High density magmatic material underplating parts of the crust
U-Mantle	3300	Upper mantle
Asth	3260	Asthenosphere
Localized density units of the upper and middle continental crust, on the basis of published literature and observed Bouguer anomalies	2650, 2400, 2950, 2650, 2300, 2850,	Features of the continental crust of varying densities; the lower density values represent sediments or granitic bodies, the higher density values represent ultramafic intrusions into the upper crust as a result of ancient tectonic activities

eastwards of the Laxmi Ridge and then deepens again to 35 km at the beginning of C3.

Further east over the continent, observed gravity shows a medium wavelength low, which is attributed primarily to a thickening of the crust evident in the previously mentioned receiver function and deep seismic results. The continental crust is thickest (40–41 km here) below the Western Ghats adjacent to the coast and thins to about 35 km further inland, a variation that coincides well with seismic results. Apart from just below the Western Ghats, the Moho in the model is located at depths less than or equal to a computed Airy Moho; below the Ghats the Moho is deeper, which is ascribed to internal loading due to the intrusion of magmatic material seen in the model. In addition to crustal thickening, near-surface, low-density material (2400 kg m^{-3}) to depths of 2–3 km, interpreted as a sedimentary basin below the Traps, is necessary to explain the large magnitude of the gravity low. The increase of the gravity response to the east of this low is similarly not fully explained by the shallowing of the Moho, as per seismic information, but requires additional high-density material at mid-crustal levels. In this model, we envisage an intrusion of C2 into C1, but it is possible that this excess mass is shallower or deeper. In the absence of substantial evidence, the exact location of this excess mass cannot be constrained. The pseudo-logs do not show evidences of a velocity inversion but this could be due to the fact that the velocity information is from a profile about 15 km to the north and nothing is available nearer at hand.

At the surface, 1-km-thick Trp (2740 kg m^{-3}) near the coast thins further inland. Fig. 4(c) shows the LAB to vary smoothly from 85 km below oceanic crust to 122 km at the ocean–continent boundary and 132 km below continental crust. This geometry is achieved by iterative modelling of this interface with a density contrast of -0.04 g cm^{-3} after incorporation of the other layer geometries according to available constraints.

4.3.2 Profile P2 (11.9° N; 1300 UTM in IGMAS)

Profile P2 (Fig. 5) is representative of the southern non-volcanic margin. The crustal layers are similar to those in P1. Seismic information in the offshore parts of this section is derived from regional multichannel seismic reflection traverses (Subrahmanyam *et al.* 1995; Chaubey *et al.* 2002) and representative pseudo-logs are shown along the section. Over the oceanic crust, the sediment thickness conforms to that of the constraining values. The Moho is at a depth of 13 km in accordance with the average thickness of oceanic crust (Figs 5a and b). The beginning of the transition zone corresponds with a strong gradient in the gravity field. The gravity low over the western parts of the transition zone coincides with the emplaced volcanic material (density 2660 kg m^{-3}) of the Chagos–Laccadive Ridge and a corresponding sag in the Moho to depths of 24 km. This density is derived from seismic velocities, which vary between 4.0 and 5.0 km s^{-1} in this region. This is lower than the density adopted for magmatic material in the northern part of the margin, which is taken as 2740 kg m^{-3} based on average of density measurements made on land. Over the Chagos–Laccadive Ridge the sediment layer thins out and thickens again further eastwards towards the coast, as is evident in seismic results from Thakur *et al.* (1999). Below these thick sediments, the Moho is subhorizontal at depths of about 28–29 km and then deepens steeply to depths of 35 km and more at the boundary between transitional and continental crust.

Und-pl at the base of the transitional crust is constrained by seismic velocity values and underlies the emplaced magmatic material of the Chagos–Laccadive Ridge near the surface. Computations indicate that this material probably does not extend beneath the continental crust.

Onshore, information from the Kavali–Udipi section, marked as III in Fig. 2(b), is incorporated in the vertical planes to the north and these geometries are carried southwards with adjustments that are required to fit the computed data to the observed gravity anomalies. Over the continent, the gravity shows a low over this region. This part of the continent is an Archaean cratonic unit and crustal thickening is commonly associated with such old continental masses. However, Moho depths of 45 km could not account for the magnitude of the low. Information from the Kavali–Udipi seismic profile, as mentioned above, does not encourage a further increase in Moho depths. Therefore, in the context of the extensive supracrustals of

greenstone–granite terrains and TTG gneisses forming the basement in this northern part of the Western Dhawar Craton, just south of Deccan Volcanic Province (Bhaskar Rao *et al.* 1991), an alternative, more plausible structure was incorporated into the model: that is, an upper crust C1 of average low density (2650 kg m^{-3}) along with a Moho at about 42 km depth. Minor near surface low-density bodies explain the shorter wavelength lows. Further south, C1 again has a normal crustal density of 2700 kg m^{-3}.

The geometry of the LAB varies from 85 km below the ocean, then rises to 67 km below the Chagos–Laccadive Ridge in the transitional zone, dips again to 140 km at the continent–ocean boundary and deepens further to 158 km below the continent. Assuming that the Moho geometry described above is the optimum geometry, the inferred geometry of the LAB (Fig. 5c) also reflects the 3-D nature of the model. Without substantial thinning of the lithosphere below the Chagos–Laccadive Ridge, the Moho would need to be as deep as 32–33 km. When the tectonic history of the region is considered, the current model with a transitional crust of medium thickness and a thinning of the lithosphere below the Chagos–Laccadive Ridge is more appropriate.

5 RESULTS FROM 3-D MODELLING

The observed and calculated gravity fields are presented in Figs 2(b) and 3(a), respectively. Visual analysis of the observed and modelled fields indicates the degree of fit that was possible given the vastness of the study area and the complexities of the geotectonic regimes. All the major highlighted Bouguer gravity lows and highs are reflected in the modelled gravity field, which indicates that it has been possible to achieve consistency in the mathematical computations, even while honoring the continuity of the geological features. This in itself indicates the potential of 3-D density modelling to depict the Earth's internal structure. To help illustrate the consistency of observations and modelled results, the coastline, outline of Laxmi Ridge, continent–ocean boundary and oceanic magnetic anomalies are marked on the maps described in more detail below (Figs 6–8).

5.1 Variations in lithospheric thickness

Fig. 6 shows the lithospheric thickness map of the region. The lithosphere–asthenosphere boundary (LAB) follows the long-wavelength dip of the crust-mantle boundary from the west to east, from a depth of 70 km in the west beneath oceanic crust to about 130 km at the continent–ocean boundary. Under the Chagos–Laccadive Ridge, the depth to the LAB is similar to the depth below the ocean basin (∼65 km). It is to be noted that instead of this localized prominent shallowing, the gravity low BGl5 could also be explained by a combination of a gentler rise of the LAB along with a local decrease in density to about 3240 kg m^{-3}. We keep to the former alternative, as we have no constraints to define this possible low-density zone.

In the transitional zone, the LAB flattens out in northern part of the margin (but has a depth comparable to that in the south between Chagos–Laccadive Ridge and coast) then deepens towards continent. The depth to the LAB increases from south to north over the continental lithosphere, which may reflect the effect of the hotspot at its base, as this part of the landmass is likely to have been in contact with the hotspot that caused the Deccan volcanism. A sensitivity analysis of the depth to the LAB reveals that the estimated thickness may vary by +/− ∼5 per cent without causing changes in the gravity response. Larger changes of LAB geometry cause changes in the gravity response that are not possible to accommodate by reasonable variations in the crust-mantle boundary and/or density.

5.2 Variations in crustal thickness

Fig. 7 shows that the crustal thickness exhibits marked variations throughout the model region. In offshore areas, the crust is thinnest (6–7 km) in the extreme southwestern corner. Below the Chagos–Laccadive and Laxmi Ridges, crustal thickening is evident; the crustal column extends to depths of 29 and 24 km, respectively. The crust of the Laxmi Basin is about 12–14 km thick. The thickness of the continental crust varies from 30–35 km at the coast to a maximum of 42–46 km below the peaks of the Western Ghats, thinning again to an average of 36 km in the east.

5.3 Magmatic underplating below the crust of the transitional zone

The presence of underplated material in the form of a high-density layer in the lower crust of the aseismic ridges and the transitional-stretched continental crust is consistent with the theory of emplacement of such a feature. Crustal underplating has been inferred in southeast Greenland along the track of Iceland hotspot and on the northwest Australian margin, (Menzies *et al.* 2000 and references therein) as well as on the Vøring volcanic passive margin offshore mid-Norway, NE Atlantic (Mjelde *et al.* 2002). Magmatic underplating may imply multiple igneous intrusions or single magma bodies, which is not resolvable in our model. The underplate body in our model, Und-pl, has been included on the basis of distinctive high-seismic velocity (>7.1 km s^{-1}) and associated gravity anomalies reported in localized regions under the Laxmi Ridge (Talwani & Reif 1998) and the central near-shore region (Udintsev 1975). The spatial extent of this body was delineated on the basis of density modelling (Fig. 8a) and the extent also correlates with the gradients shown in Fig. 2(c). The model was run with and without the Und-pl body and the difference in the corresponding Bouguer anomalies varied between −2 and −12 mGal (Fig. 8b). To account for these variations, the depths of the crustal layers needed to be increased unrealistically by 4–5 km. This increase is not supported by any seismic data.

The maximum thickness of the inferred underplated body is as much as 6 km. Below the crust of the Laxmi Basin, the underplated material is reduced to negligible thickness to match the observed fields. The underplated material at the base of the crust is found to be of significant thickness (3 km on average) in the northern part of the model below the Laxmi Ridge and the northwestern edge of the continent (Fig. 4). In the south, significant thickness is found only below the Chagos–Laccadive Ridge and the underplate does not extend into the continental crust (Fig. 5). This inference is in accordance with seismic surveys over other major hotspot tracks in the Indian Ocean or at Reunion (Charvis *et al.* 1999; Grevemeyer *et al.* 2001). Underplating is prominent in the northern offshore under the Laxmi Ridge and extending below the continental crust where the Reunion plume interacted directly with the continental crust and the Deccan Traps indicate substantial magmatic activity.

5.4 Variations in offshore sediment thickness

Fig. 9 shows a sediment thickness map of the offshore area, an important contribution of the density model, which has been constrained by global and local information, as discussed in Section

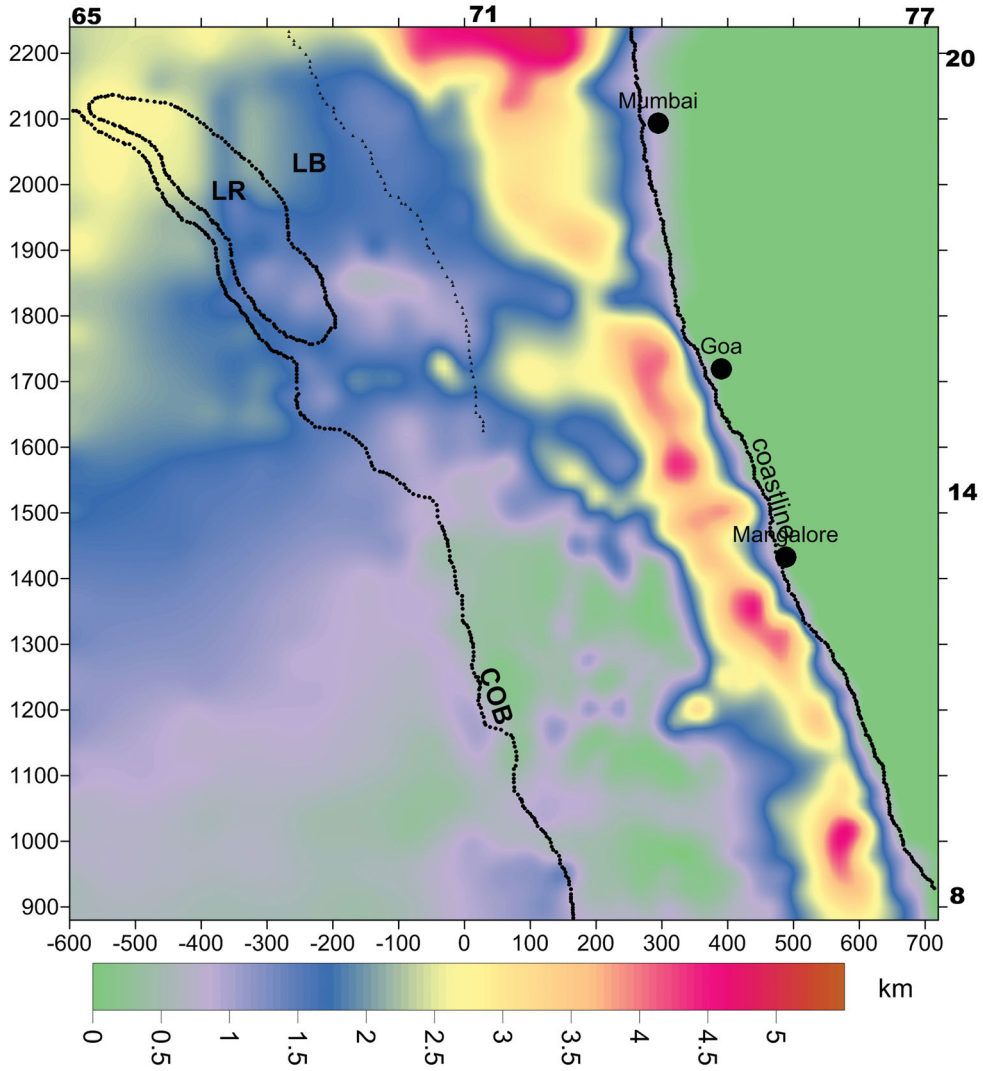

Figure 9. Sediment thickness from the 3-D density model. The outline of Laxmi Ridge and Laxmi Basin, coastline, COB, alternate COB and the vertical sections P1 and P2 are marked.

4.2. In the south, in the Arabian Sea abyssal plains and over the Chagos–Laccadive Ridge, the sediment thickness is negligible. This increases to the north to between 1.5 and 2.5 km. This is due to the influx of sediments from the Indus plains, which can be traced just offshore Mumbai, where the thickness is about 4.5 km. All along the shelf region, the sedimentary thickness varies from 2.5 to 4.5 km on average. Results from a recent seismic investigation in the southern part of the WCMI indicate an average sediment thickness of 2–2.5 km in this area (DGH 2006), which matches remarkably well with the results of the density model. This section also corroborates the lateral crustal variations in terms of continental crust to the east, transitional crust in the centre and oceanic crust to the west of the Chagos–Laccadive Ridge. To a depth of 5 km, no significant volcanic extrusive bodies are evident in this section.

6 DISCUSSION

The 3-D lithospheric model provides the subsurface structure, however, the evolution of these variations is much more complex. In general, volcanic rifted margins evolve by a combination of extrusive flood volcanism, intrusive magmatism, extension, uplift and erosion. The temporal and spatial relationships between these processes are influenced by the plate tectonic regime: the pre-existing lithosphere (thickness, composition, geothermal gradient), the upper mantle (temperature and character), the magma production rate and the prevailing climatic conditions. The magmatic and structural evolution of individual rifted margins is complex and may not fit simple models due to the geology, age and thickness of the pre-rift lithosphere and proximity to plume heads, which are potentially variable in temperature, longevity and dimensions. There may be a gradation from volcanic rifted margins to non-volcanic ones; a possible continuum appears to exist in the Red Sea (Banda *et al.* 1995 and references therein). Lithospheric thinning is a basic requirement for passive margin formation. More controversial is the mechanism responsible for the production of large volumes of basaltic volcanism at the Earth's surface and the conditions and processes which control the nature of a margin, volcanic or non-volcanic. Flood volcanism could be thick (7 km in Greenland) or relatively thin (1.5 to 2 km in the Deccan), magmatism can pre-date breakup by several million years, magmatism and breakup can be synchronous or it can post-date breakup by several million years. Some of these issues are discussed below for the WCMI, based on the 3-D model described above.

6.1 Volcanic and non-volcanic parts of the passive WCMI

Lithospheric thinning is an integral part of the architecture of passive rifted margins like the WCMI. Although crustal underplating is a common characteristic of volcanic margins along with the extruded volcanic sequences, the lack of pre- and synrift volcanics is a classic non-volcanic margin characteristic. Seaward-dipping reflector sequences which steepen and diverge downward with dips of over 15 degrees, first recognized along the North Atlantic margin (Menzies *et al.* 2003), are signatures of volcanic rifted margins. These reflectors are interpreted to be largely subaerial eruptions, and their seaward termination may typically mark the transition to submarine eruptions.

Our density model indicates lithospheric thinning in the transition as well as continental regions in the north (75–125 km) and thinning below the Chagos–Laccadive Ridge (65–70 km) at the western edge of the transition zone in the south. The model elucidates distinct differences between the northern and southern WCMI, approximately segmented at about 15°N. It suggests a heavily reworked and deformed continental crust in the northern part, which has resulted in an extended transition zone with large variations in crustal geometry and densities of intrusives in different parts of the transition zone. This is absent in the southern part, suggesting that the northern and southern parts have evolved differently (refer to the vertical sections in Figs 4 and 5). This notion is also supported by the presence of seaward dipping reflectors reported off the continental shelf of Saurashtra (Hinz 1981), north of the study area.

Some workers (Sheth 1999) have proposed that the large magmatic emplacement of Deccan volcanism is a consequence of sheared mantle in a rift setting, which might also have resulted in intrusion of high-density material at the base of the crust. It is also a contention that the magnitude and nature of melt generation is linked with the temperature of the underlying mantle of passive margins (Péréz-Gussinyé & Reston 2001; Reston & Phipps Morgan 2004). It is suggested that the mantle temperatures in the northern parts of the WCMI was higher by 200 °C at the time of rifting on the basis of rare earth element inversion studies (Armitage *et al.* 2010). Therefore, we consider it is more likely that the high-density material at the base of the crust is a result of underplating associated with the large magmatic eruptions of Deccan volcanism that reworked the crust in this region. Interpretation of gravity and magnetic data has similarly led to the inference of magmatic underplating in the Western Siberian Basin, which is another large igneous province (Braitenberg & Ebbing 2009). In the southern part of the WCMI, there is not enough evidence to support a margin of volcanic nature though there are reported limited exposures of volcanic rocks in the St. Mary's Islands (SMI; Valsangkar *et al.* 1981).

6.2 Formation of transitional crust off the western continental margin of India

The density model exhibits a transition zone, wider in the north and narrower in the south, which has density and thickness values intermediate between the oceanic and continental lithosphere. We infer that this is largely the consequence of stretching of the continental crust in an extensional environment, further intruded by material from the upper mantle as well as oceanic crust. It bears the imprints of the various tectonic activities that have influenced it.

The whole of the transition zone is underlain by magmatic material (Fig. 8a); only in the area of the Laxmi Basin it is significantly reduced in thickness. We suggest that the transitional crust, with the magma underplate thickening its base, between the offshore ridges and the continent simply stretched and lengthened under the influence of hotspot activity. The underplate is absent below the oceanic crust; there is no evidence of compatible velocity structures over the ocean basin in the entire region. Francis & Shor (1966) and Babenko *et al.* (1981), based on seismic refraction studies and CDP shooting, suggested that the Chagos–Laccadive Ridge forms a transition between the continental crust on the east and the oceanic crust on the west. Our model supports this idea and shows the base of the Chagos–Laccadive Ridge to be affected by underplating. We infer that the Chagos–Laccadive Ridge represents the effect of the interaction of the Reunion plume on the edge of the transitional crust, giving way to normal oceanic crust to the west. The results of the Ocean Drilling Program (ODP) Leg 679 115 (Fisk *et al.* 1987; Gupta *et al.* 2010) and the isostatic response of the ridge (Tiwari *et al.* 2007) support the idea that the Chagos–Laccadive Ridge is a linear volcanic feature formed over a nascent/rifted margin during the northwards motion of the Indian Plate over the Reunion hotspot.

6.3 Laxmi Ridge and Laxmi Basin

The area between the continental shelf and the Laxmi Ridge (i.e. the Laxmi Basin) is a key feature in deciphering the tectonic evolution of the northeastern Arabian Sea that was adjacent to the continent before the Deccan volcanism caused by the Reunion plume. The oldest seafloor spreading anomaly in the Arabian Sea is anomaly #27, and hence the seafloor here formed at about 61 Ma (Müller *et al.* 2001). Bhattacharya *et al.* (1994), Talwani & Reif (1998), Radha krishna *et al.* (2002), have forwarded the idea that the crust beneath Laxmi Basin is oceanic, in which case a possible alternate continent–ocean boundary in the north could be along the line with '?' marks in Figs 2(a) and (b), as well as subsequent figures. Fig. 2(c) also indicates a continuous gradient trend along this axis. More recently, Armitage *et al.* (2010) infer Laxmi Basin to have oceanic crust; Calvès *et al.* (2011) have also argued that the Gop Rift in the northern part of Laxmi Basin started opening at ∼71 Ma and continued into the Laxmi Basin. However, other studies show that the magnetic anomalies may be caused by dykes or intrusions and thus support rifting, but not necessarily seafloor spreading (Miles *et al.* 1998; Krishna *et al.* 2006). On the basis of our density model, we prefer to interpret this as thinned continental crust.

In terms of topography of the basement, the Laxmi Basin does not mimic the typical features of other extinct spreading ridges that are generally characterized by wide median valleys (Osler & Louden 1995; Grevemeyer *et al.* 1997). In contrast, the Laxmi Basin shows a prominent ridge approximately in the middle of the small basin (Talwani & Reif 1998). Moreover, if the extent of the Laxmi Basin is used to estimate spreading rate, it would be much lower (less than 1.0 cm yr^{-1}) than the rates of spreading observed elsewhere in the Arabian Sea (Bhattacharya *et al.* 1994).

The 3-D gravity model indicates a continental-type crust for the Laxmi Ridge. The crust is up to 20 km thick, including a 4–5 km thick layer of underplated material. It is complicated to date underplated material in the lower crust, but it is difficult to accept that the underplated layer in the western margin and Laxmi Ridge is unrelated and thus we infer that the underplated layer beneath Laxmi Basin was simply the result of stretching and thinning under the continued influence of the thermal anomaly which was the cause of the Deccan eruptions. The crust under Laxmi Basin is thinned to ∼10–12 km, including <1 km of underplated material. In terms of the crustal thickness, the crust could be oceanic as about 10-km-thick crust is reported under the Gop Rift (Minshull *et al.* 2008).

Although oceanic crust of a similar age to the Deccan volcanism (∼65 Ma) could be another possibility (Collier *et al.* 2008), it may also be noted that the 3-D model does not indicate any localized lithospheric thinning under Laxmi Basin (Fig. 6). Such thinning would be expected if there was oceanic crust under the basin. The ocean depth is also not compatible with the reported age based on magnetic anomalies.

Based on the above information, we prefer to interpret the Laxmi Basin as extended continental crust because if seafloor spreading in the basin occurred before Deccan volcanism, we would expect the plume to have caused significant underplating beneath the Laxmi Basin crust, as is the case for the Laxmi Ridge where underplated material was emplaced at the time of Deccan Volcanism. However, our 3-D model does not indicate significant underplating beneath the Laxmi Basin. This in turn suggests that the Laxmi Basin formed after the Seychelles drifted away from the Laxmi Ridge as a part of multiple continental breakup events, though it is difficult to estimate the time the formation of the Laxmi Basin from this study.

Analyses of well data on the western Indian shelf suggest anomalous subsidence of most seaward sites that took place as recently as late Oligocene to early Miocene. This recent subsidence is explained by a combination of thermal subsidence, flexural effects of Indus fan loading, as well as flexural effects associated with 'rapid growth of the continental margin' (Whiting *et al.* 1994). We interpret this evidence to be supportive of our idea of formation of the Laxmi Basin after the Deccan volcanic episode. The continued evolution of the Laxmi Basin might even be as young as the Indo/Eurasia collision.

6.4 Chagos–Laccadives ridge in the WCMI

After the Deccan Volcanic Province was formed, India moved northeastwards and hence away from the hotspot source. At roughly 62 Ma, the hotspot started to interact with the southern edge of the western margin. Here, the interaction between the rising plume material and the continental block occurred near the westernmost edge of the continent/ocean transitional zone, perhaps due to the obstruction presented by the thick lithosphere of the Western Dharwar Craton (Raval 2003). In Fig. 1(a), the ages of rocks in the middle and southern parts of the Chagos–Laccadive Ridge are shown in brackets (Duncan & Hargraves 1990). The Chagos–Laccadive Ridge exhibits subdued magnetic anomalies over its eastern half, whereas over the western half, several high-amplitude anomalies are to be seen (Bhattacharya *et al.* 1992). Today, the Chagos–Laccadive Ridge to the north of latitude 8°N approximates the boundary between the Indian continent and the oceanic basin.

6.5 Variations along the WCMI

Across the WCMI, the geometries of the lithosphere, crust and underplated material are depicted from north to south (Figs 6, 7 and 8a). The transition zone is much wider in the north with an average crustal thickness of 14 km in the west, increasing gradually to 22 km in the east and about 30 km at the coastline. In the south, the crustal thickness in offshore areas is about 6–7 km on an average, with a sharp gradient at the boundary of the transitional zone where it increases to 20 km and more. At the coastline, the crust is about 32 km thick. The change in lithospheric thickness from west to east is gentler in the northern part, suggesting the fact that the entire region was affected by the presence of the Reunion plume. On the other hand, the gradients in the LAB are again sharp in the south. This is ascribed to the fact that the continental part here remained unaffected due to its path of movement, whereas the immediate offshore interacted with the hotspot.

6.6 Suggested evolutionary model

Over several decades, numerous results from diverse techniques and data sets in different parts of the Arabian Sea have led to different models for the evolutionary history of the region. Apart from the classical interpretations carried out by earlier workers, interesting results are presented in recent studies (Collier *et al.* 2008, 2009; Minshull *et al.* 2008; Armitage *et al.* 2010; Corfield *et al.* 2010; Calvès *et al.* 2011). Collier *et al.* (2008) concluded that the Laxmi Ridge is heavily intruded thinned continental crust and that the separation of the Seychelles from India was completed by 62 Ma; that is, after the Deccan volcanism episode. On the other hand, Calvès *et al.* (2011), based on a variety of geophysical and geological observations, including detailed volcanostratigraphy on each part of seismic sections, as well as Corfield *et al.* (2010) believe the separation of the Seychelles and India was complete at around 65 Ma; that is, contemporaneously with the Deccan volcanism and the Laxmi Basin formed as an aborted rift and associated oceanic crust. The seismic velocity structure of the Laxmi Basin is comparable with that of the Laxmi Ridge, Seychelles Bank and western part of the Indian continental shield. Krishna *et al.* (2006) also suggested that Laxmi Basin and Laxmi Ridge are reworked continental crust. On the basis of interpretation of seismic data and numerical modelling of melt generation, Armitage *et al.* (2010) suggested that Laxmi Ridge and Seychelles margin separated before Deccan volcanism and modest magmatic intrusion under Laxmi Ridge is a consequence of partial depletion of the thermal anomaly resulting from this process. Thus, there is continuing controversy on the nature of the crust of the Laxmi Ridge and Laxmi Basin, as well as on the relative sequence of events that lead to the formation of these two features.

From the regional 3-D architecture represented in our density model, it is possible only to put relative time constraints on the major sequence of tectonic events. The geometry of the crust, mantle and asthenosphere, which is the result of comprehensive 3-D density modelling, leads us to advocate the following: (1) separation of Madagascar from combined India/Seychelles (∼90–88 Ma); (2) around 68–65 Ma, subsequent to the formation of the failed Gop Rift, separation of the Seychelles from India and formation of Laxmi Ridge during Seychelles breakup, immediately followed by Deccan volcanism and (3) stretching of continental lithosphere to form the Laxmi Basin followed by emplacement of the Chagos–Laccadive Ridge at the southern edge of the northward-moving continental margin. Thus, we suggest that both the Laxmi Ridge and Laxmi Basin are continental in origin and are constituents of the broad transitional crust of this part of the WCMI.

Though it is difficult to refute the oceanic nature of the Laxmi Basin on the basis of gravity data alone, it is also difficult to accept that the hotspot did not alter the nascent transitional crust of the Laxmi Basin or that all the signatures of magnetic anomalies from the original oceanic crust have remained unaltered. Also, on the basis of similar thickness of underplated material below the Laxmi Ridge and the then adjoining Deccan Volcanic Province, we believe that they formed at the same time. Thus, the intervening Laxmi Basin crust could only have formed at a later stage with the stretching and thinning of the transitional continental crust. This also explains why the thickness of the underplated material in this part is negligible. Such a model is also analogous to the conclusions of recent studies (Krishna *et al.* 2006; Collier *et al.* 2009).

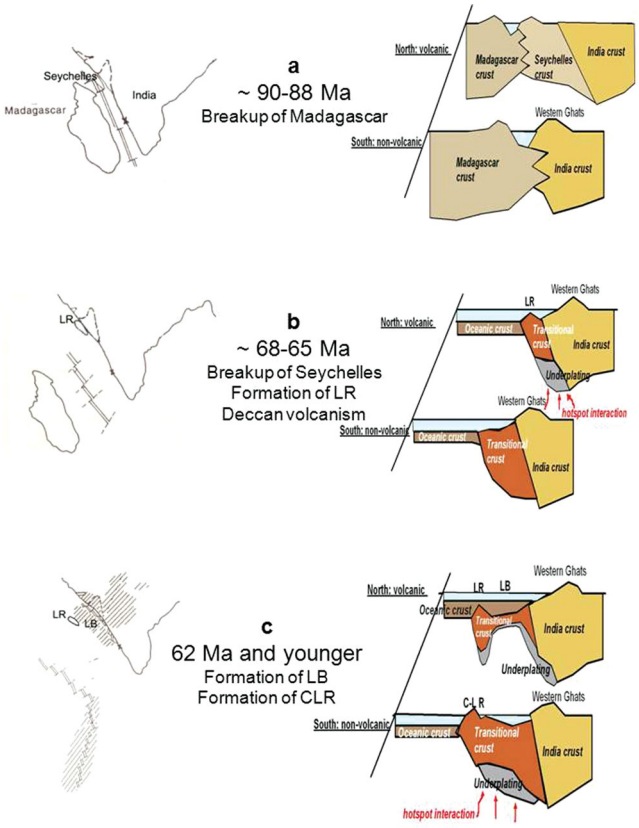

Figure 10. Schematic diagram of the evolution of the passive continental margin of India showing the suggested timing of the main events as compiled from various sources mentioned in text. Representative vertical sections are presented for three different times: (a) −90 to 88 Ma: showing the rifting of Madagascar from the Indian Peninsular Shield in the south and from Seychelles in the north with the concurrent opening of the Arabian Sea. (b) −68 to −65 Ma: earlier rifting leads to the formation of the transitional crust in the south, whereas in the north, fresh asthenospheric upwelling/rifting associated with Reunion hotspot leads to drifting of Seychelles and formation of Laxmi Ridge (LR). This is accompanied by massive surface extrusions (not evident at this scale) and underplating of continental and oceanic crust. (c) –62 Ma and younger: post-Deccan volcanism episode, the Laxmi Basin (LB) is formed in stretched and downfaulted continental crust in the north and Chagos–Laccadive Ridge (CLR) is formed on the edge of continental crust in the south as the Indian continent moves across the Reunion hotspot in a NNE direction. The hachured areas in the map indicate the regions which saw outpourings of mantle material associated with Deccan volcanism as surface extrusions and/or underplated material.

Apart from the configuration of the Laxmi Ridge and Laxmi Basin, our model of the 1200 km length of the WCMI shows a distinct difference in the northern part where the lithosphere–asthenosphere boundary show gradual change and in the southern part where the same shows an abrupt shallowing below the Chagos–Laccadive Ridge. This leads us to invoke the two-stage evolutionary hypothesis of the WCMI. The first phase was passive and non-volcanic, and is commonly associated with the influence of the Marion hotspot. The second stage is attributed to the Reunion plume and is active and volcanic in nature, resulting in extensive outpourings of the Deccan Traps in the northern part of the margin.

Fig. 10(a) shows the passive rifting of Madagascar, which was attached to India (except in the north where it adjoined the Seychelles) and the formation of the Western Ghats escarpments and topography of the Seychelles and opening of the Arabian Sea at about 90 Ma.

Fig. 10(b) shows the margin at about 68–65 Ma, before the Deccan volcanic episode when the region experienced the effects of renewed hotspot activity associated with the Reunion hotspot in the northern part of the margin. The breakup of Seychelles commenced at this time, if not by active rifting associated with formation of the Gop Rift, then, as there are no signatures of rifting in the LAB, possibly by asthenospheric upwelling associated with the Reunion hotspot. The drifting away of the Seychelles and the eastward jump of the spreading ridge is accompanied by downwarping of a part of the Indian continental crust and possibly further northward extension of the Western Ghats. The downwarped piece of the Indian margin in the north formed the topography of Laxmi Ridge at the western edge of the transitional zone. At the same time, massive extrusions from the Reunion plume spread over the continent in the north as well as offshore over the Laxmi Ridge in the form of Deccan Traps (it is not possible to show this thin layer of basalts which covered the surface, in the diagram). Underplating of plume-generated material at the bottom of the crust also takes place in the same region. In the southern part of the margin, a transition zone is formed as a remnant of the Madagascar rifting episode.

Fig. 10(c) depicts the post-Deccan volcanism scenario at about 62 Ma and younger when the Indian landmass moved to the north and east, stretching gave rise to the Laxmi Basin in the north and the interaction of the Reunion plume with the edge of the transitional crust led to the emplacement of the Chagos–Laccadive Ridge along with crustal underplating in the southern part of the margin.

7 CONCLUSIONS

The 3-D density model has enabled us to infer the regional configuration of the WCMI in terms of variations in crust-mantle and lithosphere–asthenosphere boundaries. The model highlights several salient features of critical interest; that is, the crust–mantle boundary varies in the southwestern corner from 13 km below the ocean to 42 km below the continental craton; below the offshore ridges the Moho dips to depths of about 23 km or more; on the continent, the Moho is at about 32 km depth at the coast, deepens to 46 km below the Western Ghats and the Nilgiris and shallows further east to an average of 35 km; the LAB has a smoother gradient from about 85 km depth in the southwestern corner to about 165 km below the cratonic interior. The extent of volcanic material is mapped offshore and onshore. It is manifested on the surface as the Deccan Volcanic Province with westward extension submerged in sea water and also as underplated material at the base of the crust.

The salient stages of the tectonic history of the WCMI, as inferred from the 3-D model, highlight primarily the effects of the different phases of rifting and hotspot interaction on the oceanic, transitional and continental crust. Through the proposed evolutionary model, we venture to say that the formation of the Laxmi Ridge and later the Laxmi Basin were the consequences of the interaction of the Reunion plume with a sunken portion of the crust at the edge of the continental, whereas the Chagos–Laccadive Ridge was formed by volcanic material from the same plume on the edge of already stretched and thinned transitional crust. This inclusive unified picture is an important contribution of this work.

This reconstruction of the sequence of events that we present to explain the 3-D model of the Western Margin is of course greatly influenced by contemporary models and hypotheses on the evolution of the western Indian passive margin and is, therefore, prone to changes as these ideas evolve in accordance with new data and

interpretation. Nevertheless, we believe that this work contains valuable information on the geometry, physical properties and the tectonic structures associated with the formation of the western continental margin of India.

ACKNOWLEDGMENTS

We are grateful to the Director, CSIR-NGRI, for his encouragement and support and permission to publish this work. Part of this work was carried out under an Indo-German Bilateral Cooperation in Science and Technology (BMBF-DLR grant IND 02/001). Thanks are due to Prof. H.-J. Götze and Dr. Sabine Schmidt for the use of the IGMAS software. We also thank Dr. K.S. Krishna for discussions on the evolution of the Laxmi Basin. The exhaustive reviews by Michel Diament, Ron Hackney and Carla Braitenberg improved the work considerably and are gratefully acknowledged.

REFERENCES

Andersen, O.B. & Knudsen, P., 2001. Global Marine Gravity Field from the ERS-1 and Geosat geodetic mission altimetry, *J. geophys. Res.,* **103**(C4), 8129.

Armitage, J.J., Collier, J.S. & Minshull, T.A., 2010. The importance of rift history for volcanic margin formation, *Nature,* **465,** 913–917.

Babenko, K.M., Panaev, V.A., Svistunov, Y.I. & Schlezinger, A.E., 1981. Tectonics of the eastern margin of the Arabian Sea according to seismic data, *Bull. ONGC,* **18,** 37–62.

Banda, E., Torné, M. & Talwani, M., 1995. Rifted ocean-continent boundaries, NATO ASI Series C, 463.

Bhaskar Rao, Y.J., Naha, K., Srinivasan, R. & Gopalan, K., 1991. Geology, geochemistry and geochronology of the Archaean Peninsular Gneiss around Gorur, Hassan district, Karnataka, India, *Proc. Indian Acad. Sci. Earth planet Sci.,* **100,** 399–412.

Bhattacharya, G.C., Chaubey, A.K., Murty, G.P.S., Srinivas, K., Sarma, K.V.L.N.S., Subrahmanyam, V. & Krishna, K.S., 1994. Evidence for seafloor spreading in the Laxmi Basin, north eastern Arabian Sea, *Earth planet. Sci. Lett.,* **125,** 211–220.

Bhattacharya, G.C., Chaubey, A.K., Murty, G.P.S., Scherbakov, V.S., Lygin, V.A., Philipenko, A.I. & Bogomyagkov, A.P., 1992. Marine magnetic anomalies in the north eastern Arabian Sea, in *Oceanography of the Indian Ocean,* pp. 503–509, ed. Desai, B.N., Oxford and IBH, New Delhi.

Biswas, S.K., 1987. Regional tectonic framework, structure and evolution of the western marginal basins of India, *Tectonophysics,* **135,** 307–327.

Bowin, C., 1983. Depth of principal mass anomalies contribution to the Earth's geoidal undulations and gravity anomalies, *Mar. Geod.,* **7,** 61–100.

Braitenberg, C. & Ebbing, J., 2009. New insights into the basement structure of the west-Siberian basin from forward and inverse modelling of Grace satellite gravity data, *J. geophys. Res.,* **114,** B06402, doi:10.1029/2008JB005799.

Calvès, G., Schwab, A.M., Huuse, M., Clift, P.D., Gaina, C., Jolley, D., Tabrez, A.R. & Inam, A,, 2011. Seismic volcanostratigraphy of the western Indian rifted margin: the pre-Deccan igneous province, *J. geophys. Res.,* **116,** B01101, doi:10.1029/2010JB000862.

Charvis, P. *et al*., 1999. Spatial distribution of hotspot material added to the lithosphere under La Réunion, from wide-angle seismic data, *J. geophys. Res.,* **104**(B2), 2875–2894.

Chaubey, A.K., Gopala Rao, D., Srinivas, K., Ramana, M.V. & Subrahmanyam, V., 2002. Analyses of multichannel seismic reflection, gravity and magnetic data along a regional profile across the central-western continental margin of India, *Mar. Geology,* **182,** 303–323.

Collier, J.S., Sansom, V., Ishizuka, O., Taylor, R.N., Minshull, T.A. & Whitmarsh, R.B., 2008. Age of Seychelles-India breakup, *Earth planet. Sci. Lett.,* **272,** 264–277.

Collier, J.S., Minshull, T.A., Hammond, J.O.S., Whitmarsh, R.B., Kendall, J.M., Sansom, V., Lane, C.I. & Rumpker, G., 2009. *J. geophys. Res.,* **114**(B3101), doi:10.1029/2008JB005898.

Corfield, R.I., Carmichael, S., Bennet, J., Akhter, S., Fatimi, M. & Craig, T., 2010. Variability in crustal structure of the Western Indian continental Margin in the Northern Arabian Sea, *Petrol. Geosci.,* **16,** 257–265.

Courtillot, V., Besse, J., Vandamme, D., Montigny, R., Jaeger, J.-J. & Cappatta, H., 1986. Deccan flood basalts and the Cretaceous-Tertiary boundary, *Earth planet. Sci. Lett.,* **80,** 361–374.

De Bremaecker, J., 1985. *Geophysics: The Earth's Interior,* p. 342, John Wiley and Sons, New York, NY.

DGH, 2006. Directorate of Hydrocarbons (Under Ministry of Petroleum and Natural Gas, Govt of India), Annual Report.

Divins, D.L., 1990. NGDC Total Sediment Thickness of the World's Oceans and Marginal Seas.

DSDP, 1974. *Initial Reports of the Deep Sea Drilling Project,* pp. 509–519, US Govt printing office, Washington, DC.

Duncan, R.A. & Hargraves, R.B., 1990. 40 Ar/39 Ar geochronology of the basement rocks from the Mascarene Plateau, the Chagos Bank and the Maldives Ridge, *Proc. ODP Sci. Results,* **115,** 43–51.

Dziewonski, A.M. & Anderson, D.L., 1981. Preliminary reference Earth model, *Phys. Earth planet. Inter.,* **25,** 297–356.

Fisk, M.R., Duncan, R.A., Baxter, A.N., Greenough, J.D., Hargraves, R.B., Tatsumi, Y., Shipboard Scientific Party, 1987. Reunion hotspot magma chemistry over the past 65 m.y.: results from Leg 115 of the Ocean Drilling Program, *Geology,* **17,** 934–937.

Francis, T.J.G. & Shor, G.G., 1966. Seismic refraction measurements in the northwestern Indian Ocean, *J. geophys. Res.,* **71,** 427–449.

Gallart, J., Driad, L., Charvis, P., Sapin, M., Hirn, A., Diaz, J., Voogd, B. & Sachpazi, M., 1999. Perturbation to the lithosphere along the hotspot track of La Reunion from an offshore-onshore seismic transect, *J. geophys. Res.,* **104,** 2895–2908.

Götze, H.-J. & Lahmeyer, B., 1988. Application of three-dimensional interactive modelling in gravity and magnetics, *Geophysics,* **56**(8), 1096–1108.

Gravity Map Series of India, 2006. Geological Survey of India and NGRI.

Grevemeyer, I., Flueh, E.R., Reichert, C., Bialas, J., Kläschen, D. & Kopp, C., 2001. Crustal architecture and deep structure of the Ninetyeast Ridge hotspot trail from active-source ocean bottom seismology, *Geophys. J. Int.,* **144,** 414–431.

Grevemeyer, I., Weiger, W., Whitmarsh, R.B., Avedic, F. & Deghani, G.A., 1997. The Aegis Rift: crustal structure of an extinct spreading axis, *Mar. Geophys. Res.,* **19,** 1–23.

Gupta, S., Rai, S.S., Prakasam, K.S., Srinagesh, D., Bansal, B.K., Chadha, R.K., Priestly, K. & Gaur, V.K., 2003. The nature of the crust in southern India: implications for Precambrian crustal evolution, *Geophys. Res. Lett.,* **30**(8), 1419–1423.

Gupta, S., Mishra, S. & Rai, S.S., 2010. Magmatic underplating of crust beneath the Laccadive Island, NW Indian Ocean, *Geophys. J. Int.,* **183,** 536–542, doi:10.1111/j.1365-246X.2010.04759.x.

Hinz, K., 1981. A hypothesis of terrestrial catastrophes—Wedge of very thick ocean wand dipping layers beneath a passive continental margin, their origin and paleo-environmental significance, *Geologische Jarnbuch,* **E22,** 3–28.

Intergovernmental Oceanographic Commission, International Hydrographic Organisation & British Oceanographic Data Centre, 1997. General Bathymetric Chart of the Oceans (GEBCO) Digital Atlas (CD-ROM), 1997 edn., British Oceanographic Data Center, Birkenhead.

Kaila, K.L. *et al*., 1979. Crustal structure along Kavali-Udipi profile in the Indian Peninsular Shield from deep seismic sounding, *J. Geol. Soc. India,* **20,** 307–333.

Kaila, K.L., Reddy, P.R., Dixit, M.M. & Lazrenko, M.A., 1981a. Deep crustal structure at Koyna, Maharastra indicated by Deep Seismic Soundings, *J. Geol. Soc. India,* **22,** 1–16.

Kaila, K.L., Murty, P.R.K., Rao, V.K. & Kharetchko, G.E., 1981b. Crustal structure from Deep Seismic Sounding along the Koyna profile II in the Deccan Trap area, India, *Tectonophysics,* **73,** 365–384.

Kennet, B.L.N. & Widiyantoro, S., 1999. A low seismic wave speed anomaly beneath north-western India: a seismic signature of the Deccan hotspot?, *Earth planet. Sci. Lett.,* **165,** 145–155.

Kolla, V. & Coumes, F., 1990. Extension of structural and tectonic trends from the Indian subcontinent into the Eastern Arabian Sea, *Mar. Petrol. Geol.,* **7,** 188–196.

Krishna Brahmam, N. & Kanungo, D.N., 1976. Inference of granitic batholiths by gravity studies in South India, *J. Geol. Soc. India,* **17,** 45–53.

Krishna, K.S., Gopala Rao, D. & Sar, D., 2006. Nature of the crust in the Laxmi Basin (14–20N), western continental margin of India, *Tectonics,* **25,** doi:10.1029/2004TC001747.

Krishna, V.G., Kaila, K.L. & Reddy, P.R., 1991. Low velocity layers in the subcrustal lithosphere beneath the Deccan trap region of Western India, *Phys. Earth planet. Inter.,* **67,** 288–302.

Kumar, A., Bhaskar Rao, Y.J., Sivraman, T.V. & Gopalan, K., 1996. Sm-Nd ages of Archaean metavolcanics of the Dharwar craton, South India, *Precambrian Res.,* **80,** 206–215.

Ludwig, W.J., Nafe, J.E. & Drake, C.L., 1970. Seismic Refraction, in *The Sea,* Vol. 4, pp. 53–84, ed. Maxwell, A.E., Wiley-Interscience, New York, NY.

Menzies, M.A., Ebinger, C. & Klemperer, S., 2000. Volcanic rifted margins, Penrose Conference Report.

Menzies, M.A., Klempere, S.L., Ebinger, C.J. & Baker, J., 2003. Characteristics of volcanic rifted margins, *Geol. Soc. Am.,* Special Paper, **362,** 1–14.

Miles, P.R., Minschy, M. & Segoufin, J., 1998. Structure and early evolution of the Arabian Sea and East Somali Basin, *Geophys. J. Int.,* **134,** 876–888.

Minshull, T.A., Lane, C.I., Collier, J.S. & Whitmarsh, R.B., 2008. The relationship between rifting and magmatism in the northeastern Arabian Sea, *Nat. Geoscience,* **1,** 463–467.

Mishra, D.C., Arora, K. & Tiwari, V.M., 2004. Gravity anomalies and associated tectonic features over the Indian Peninsular Shield and Adjoining Oceans, *Tectonophysics,* **379,** 61–76.

Mishra, D.C., Kumar, V.V. & Rajasekhar, R.P., 2006. Analysis of airborne agnetic and gravity anomalies of Peninsular Shield, India integrated with seismic and magnetolluric results and gravity anomalies of Madagascar, Sri Lanka and East Antarctica, *Gondwana Res.,* **10,** 6–17.

Mjelde, R., Kasahara, J., Shimamura, H., Kamimura, A., Kanazawa, T., Kodaira, S., Raum, T. & Shiobara, H., 2002. Lower crustal seismic velocity-anomalies; magmatic underplating or serpentinized peridotite? Evidence from the Vøring Margin, NE Atlantic, *Mar. Geophys. Res.,* **23**(2), 169–183.

Mjelde, R., Raum, T., Murai, V. & Takanami, T., 2007. Continent ocean transitions, review and a new tectono-magnetic model of the Voring Plateau, NE Atlantic', *J. Geodyn.,* **431,** 374–392.

Müller, R.D., Gaina, C., Roest, W.R. & Hansen, D.L., 2001. Á recipe for micro-continent formation, *Geology,* **29,** 203–206.

Naini, B.R. & Talwani, M., 1982. Structural frame work and evolutionary history of the continental margin of western India, in *Studies in Continental Margin Geology,* AAPG Memoir Vol. 34, pp. 167–191, eds Watkins, J.S. & Drake, C.L., American Association of Petroleum Geologists, Tulsa, OK.

NGRI, 2003. Processing and interpretation of marine geophysical data (Gravity, Magnetic and bathymetric) from five offshore blocks of western Indian continental margin of India, Technical Report no.NGRI-2003-EXP-38, (unpublished).

Osler, J.C. & Louden, K.E., 1995. Extinct spreading center in the Labrador Sea: crustal structure from a two-dimensional seismic refraction velocity model, *J. geophys. Res.,* **100**(B2), 2261–2278.

Pande, K., Sheth, H.C. & Bhutani, R., 2001. ^{40}Ar-^{39}Ar age of the St. Mary's Islands volcanics, southern India: record of India-Madagascar break-up on the Indian subcontinent, *Earth planet. Sci. Lett.,* **193,** 39–46.

Pandey, O.P., Agrawal, P.K., Singh, A.P. & Negi, J.G., 1993. Modelling of gravity field over the Laxmi Ridge and lithospheric structure, *Proceedings of the 29th Annual Convention of the Indian Geophysical Union,* 53–57.

Parida, G. & Mishra, Y.K., 1992. A late Paleocene-early Eocene Fandelta in Bombay offshore basin, *Bull. ONGC,* **29,** 109–120.

Péréz-Gussinyé, M. & Reston, T.J., 2001. Rheological evolution during extension at nonvolcanic rifted margins: onset of serpentinization and development of detachments leading to continental breakup, *J. geophys. Res.,* **106**(B3), 3961–3975.

Prasada Rao, R. & Srivastava, D.C., 1984. Regional seismic facies analysis of western offshore, India, *Bull. ONGC.,* **21**(1), 83–96.

Qureshy, M.N., Krishna Brahmam, N., Verma, R.K., Bhalla, M.S., Garde, S.C., Divakara Rao, V. & Naqvi, S.M., 1967. Geological, geochemical and geophysical studies along the 14th parallel in Mysore, *Symposium on Upper Mantle Project, Hyderabad, GRB and NGRI Publication,* **8,** 211–225.

Radha Krishna, M., Verma, R.K. & Purushottam Arts, K., 2002. Lithospheric structure below the eastern Arabian Sea and adjoining West Coast of India based on integrated analysis of gravity and seismic data, *Mar. Geophys. Res.,* **23,** 25–42.

Raval, U., 2003. Interaction of Mantle Plume with Indian Continental Lithosphere since the Cretaceous, *Mem. Geol. Soc. India,* **53,** 449–479.

Ravi Kumar, M., Saul, J., Sarkar, D., Kind, R. & Shukla, A.K., 2001. Crustal structure of the Indian shield: new constraints from teleseismic receiver functions, *Geophys. Res. Lett.,* **28,** 1339–1342.

Reston, T.J. & Phipps Morgan, J., 2004. Continental geotherm and the evolution of rifted margins, *Geology,* **32,** 133–136.

Royer, J.Y. *et al*., 1992. Indian ocean plate reconstructions since the Late Jurassic, in *Synthesis of Results from Scientific Drilling in the Indian Ocean,* Geophys. Monogr. Vol. 70, pp. 471–475, eds Duncan, R.A., Rea, D.K., Kidd, R.B., Von Rad, U. & Weissel, J.K., American Geophysical Union, Washington, DC.

Sarkar, D., Chandrakala, K., Padmavathi Devi, P., Sridhar, A.R., Sain, K. & Reddy, P.R., 2001. Crustal velocity structure of western Dharwar craton, south India, *J. Geodyn.,* **31,** 227–241.

Sarkar, D., Ravi Kumar, M., Saul, J., Kind, R., Raju, P.S., Chadha, R.K. & Shukla, A.K., 2003. A receiver function perspective of the Dharwar craton (India) crustal structure, *Geophy. J. Int.* **154**(1), 205–211.

Schmidt, S. & Götze, H.-J., 1998. Interactive visualization and modifications of 3D models using GIS functions, *Phys. Chem. Earth,* **23**(3), 289–296.

Sheth, H.C., 1999. Flood basalts and large igneous provinces from deep mantle plumes: fact, fiction and fallacy, *Tectonophysics,* **311,** 1–29.

Singh, A.P., 1999. The deep crustal accretion beneath the Laxmi Ridge in the north-eastern Arabian Sea: the hotspot model again, *J. Geodyn.,* **27,** 609–622.

Srinagesh, D. & Rai, S.S., 1996. Teleseismic tomographic evidence for constraining crust and upper mantle in south Indian Archaean Terrains, *Phys. Earth planet Inter.,* **97,** 27–41.

Storey, M., Mahoney, J.J., Saunders, A.D., Duncan, R.A., Kelley, S.P. & Coffin, M.F., 1995. Timing of hotspot-related volcanism and the breakup of Madagascar and India, *Science,* **267,** 852–855.

Subrahmanya, K.R., 1998. Tectono-magmatic evolution of the west coast of India, *Gondwana Res.,* **1**(3/4), 319–327.

Subrahmanyam, C. & Verma, R.K., 1981. Densities and magnetic susceptibities of Precambrian rocks of different metamorphic grade (southern Indian shield), *J. geophys. Res.,* **49,** 101–107.

Subrahmanyam, V., Gopala Rao, D., Ramana, M.V., Krishna, K.S., Murty, G.P.S. & Gangadhara Rao, M., 1995. Structure and tectonics of the southwestern continental margin of India, *Tectonophysics,* **249,** 267–282.

Talwani, M. & Reif, C., 1998. Laxmi Ridge—A continental sliver in the Arabian Sea, *Mar. Geophys. Res.,* **20,** 259–271.

Tapley, B. D. & Kim, M.-C., 2001. Applications to geodesy, in *Satellite Altimetry and Earth Sciences*, Int. Geophys. Ser. Vol. 69, ch. 10, pp. 371–406, eds Fu, L.-L. & Cazenave, A., Elsevier, New York, NY.

Thakur, S.S, Arasu, R.T., Subrahmanyam, V.S.R., Srivastava, A.K. & Murty, A.V.S., 1999. Basin configuration in Konkan deepwaters: western indian offshore, *J.Geol. Soc. India.,* **53,** 79–88.

Tiwari, V.M. & Mishra, D.C., 1999. Estimation of effective elastic thickness from gravity and topography data under the deccan volcanic province, India, *Earth planet. Sci. Lett.,* **171,** 189–299.

Tiwari, V.M., Grevemeyer, I., Singh, B., & Phipps Morgan, J., 2007. Variation of effective elastic thickness and melt production along the Deccan/Reunion hotspot track, *Earth planet. Sci. Lett.,* **264,** 9–21.

Tiwari, V.M., Rao, M.B.S.V. & Mishra, D.C., 2001. Density inhomogeneities beneath Deccan volcanic province, India as derived from gravity data, *J. Geodyn.,* **31,** 1–17.

Todal, A. & Eldholm, O., 1998. Continental margin off Western India and deccan large igneous province, *Mar. Geophys. Res.,* **20,** 273–291.

Udintsev, G.B., 1975. Geological and geophysical atlas of the Indian Ocean, Moscow Academy of Sciences, 151.

Valsangkar, A.B., Radhakrishnamurthy, C., Subbarao, K.V. & Beckinsale, R.D., 1981. Paleomagnetism and potassium-argon age studies of acid igneous rocks of St. Mary's Islands, *Mem. Geol. Soc. India,* **3,** 265–275.

White, R. & McKenzie D., 1989. Magmatism at rift zones–The generation of volcanic continental margins and flood basalts, *J. geophys. Res.,* **94,** 7685–7729.

Whiting, B.M., Karner, G.D. & Driscoll, N.W., 1994. Flexural and stratigraphic development of the west Indian continental margin, *J. geophys. Res.,* **99**(B7), 13 791–13 811.